THESIS FOR THE DEGREE OF DOCTOR OF PHILOSOPHY

Particulate Flows in Aftertreatment Systems

Model Development and Numerical Simulations

HENRIK STRÖM

CHALMERS

Department of Chemical and Biological Engineering
CHALMERS UNIVERSITY OF TECHNOLOGY
Göteborg, Sweden 2011

Particulate Flows in Aftertreatment Systems
Model Development and Numerical Simulations
HENRIK STRÖM
ISBN 978-91-7385-490-0

Doktorsavhandlingar vid Chalmers tekniska högskola
Ny serie nr 3171
ISSN 0346-718X

Chemical Engineering
Department of Chemical and Biological Engineering
Chalmers University of Technology
SE-412 96 Göteborg
Sweden

Telephone: +46 (0)31-772 1000

Chalmers Reproservice
Göteborg, Sweden 2011

Particulate Flows in Aftertreatment Systems
Model Development and Numerical Simulations

Henrik Ström
Chemical Engineering
Department of Chemical and Biological Engineering
Chalmers University of Technology

ABSTRACT

Emissions from internal combustion engines contain many components that have a detrimental effect on the environment and on human health, such as nitrogen oxides (NO_x) and particulate matter (PM). In addition, the final product of any combustion of fossil fuel - carbon dioxide (CO_2) - contributes to global warming. In order to reduce the emissions of CO_2, more efficient engines are needed, and these typically necessitate the development of new exhaust gas aftertreatment systems. Lean-burn engines (e.g. the diesel engine) are more efficient than conventional petrol engines, but emit more PM and require addition of a reducing agent to reduce NO_x. Usually, a urea-water solution or a hydrocarbon is sprayed into the system. In addition, the PM content of the exhaust must be reduced in terms of both mass and number.

In the current work, detailed mathematical models are used to investigate the motion and deposition of PM and droplets in generic exhaust gas aftertreatment systems. It is shown that PM from internal combustion engines can be divided into three groups depending on their size, and that these groups are transported differently in the aftertreatment system. This is reflected in the extent and location of particle deposition, and can be taken advantage of in emission control engineering. Several particle transport models of differing complexity are presented and used to study the PM trapping characteristics of a number of filter designs. Also the influence of turbulence on the transport of particulate matter and droplets in aftertreatment systems is studied by means of numerical simulations.

Finally, a model for simulations of gas-solids systems involving particles of size significant to that of the bounding geometry but also to the mean free path of the gas is presented. This very challenging flow situation is encountered inside the pores of a porous wall in a typical diesel particulate filter. It is shown that the new model can provide more accurate results than the previously available methods of similar computational cost.

Keywords: Particulate flow, Multiphase flow, Exhaust gas aftertreatment, Particulate matter, Modeling, Computational fluid dynamics

List of papers

This thesis is based on the work presented in the following papers, which are referred to throughout the text by their Roman numerals:

I. **Choice of Urea-spray Models in CFD Simulations of Urea-SCR Systems**
Henrik Ström, Andreas Lundström & Bengt Andersson
Chemical Engineering Journal **150** (2009) 69-82

II. **Simulations of Trapping of Diesel and Gasoline Particulate Matter in Flow-through Devices**
Henrik Ström & Bengt Andersson
Topics in Catalysis **52** (2009) 2047-2051

III. **Design of Automotive Flow-through Catalysts with Optimized Soot Trapping Capability**
Henrik Ström, Srdjan Sasic & Bengt Andersson
Chemical Engineering Journal **165** (2010) 934-945

IV. **A Novel Multiphase DNS Approach for Handling Solid Particles in a Rarefied Gas**
Henrik Ström, Srdjan Sasic & Bengt Andersson
Submitted to *International Journal of Multiphase Flow*

V. **Effects of the Turbulent-to-laminar Transition in Monolithic Reactors for Automotive Pollution Control**
Henrik Ström, Srdjan Sasic & Bengt Andersson
Submitted to *Industrial & Engineering Chemistry Research*

VI. **Turbulent Ceramic Diesel Oxidation Catalysts for Improved Removal of Fine Particulate Matter**
Henrik Ström, Srdjan Sasic & Bengt Andersson
In manuscript

Related works, not included in this thesis:

Numerical Simulations of Solid Particle Motion in Rarefied Flow Using VOF
Henrik Ström, Srdjan Sasic & Bengt Andersson
Proceedings of the International Conference on Multiphase Flow (2010)

Modeling of Urea Gas Phase Thermolysis and Theoretical Details on Urea Evaporation
Andreas Lundström, Björn Waldheim, Henrik Ström & Björn Westerberg
Submitted to *Journal of Automobile Engineering*

Contribution report

I. I performed all of the simulations together with Andreas Lundström, participated considerably in the evaluation of the results and wrote most of the first draft of the manuscript.

II. I performed all of the simulations and wrote the first draft of the manuscript. The design of the computational model the and evaluation of the results were performed together with my co-author.

III. I performed all of the simulations and wrote the first draft of the manuscript. I planned the simulations and evaluated the results together with my co-authors.

IV. I performed all of the simulations and wrote the first draft of the manuscript. I planned the simulations and evaluated the results together with my co-authors.

V. I performed all of the simulations and wrote most of the first draft of the manuscript. I evaluated the results together with my co-authors. The signal analysis was performed together with Srdjan Sasic.

VI. I performed all of the simulations and wrote the first draft of the manuscript. I planned the simulations and evaluated the results together with my co-authors.

List of abbreviations

CFD	computational fluid dynamics
CO	carbon monoxide
CO_2	carbon dioxide
DNS	direct numerical simulation
DOC	diesel oxidation catalyst
DPF	diesel particulate filter
DSMC	direct simulation Monte Carlo
EGR	exhaust gas recirculation
HC	hydrocarbons
H_2O	water
LES	large eddy simulation
N_2	nitrogen
NO	nitric oxide
NO_2	nitrogen dioxide
NO_x	nitrogen oxides (NO and NO_2)
PM	particulate matter
RANS	Reynolds-averaged Navier-Stokes
SCR	selective catalytic reduction
TWC	three-way catalyst

Contents

Chapter 1

Introduction

1.1 Background

The concern about air pollution and global warming has increased dramatically over the last decade. Vehicles in the transport sector, driven by fossil fuels, emit many different pollutants to the air and account for a large part of the total emissions in the EU [1] and elsewhere [2]. These emissions include carbon monoxide (CO), various hydrocarbons (HC) and also nitrogen oxides (NO_x) [3], which are all poisonous and dangerous to inhale for humans. Other effects which are highly detrimental to the environment and living organisms from these gases include acid rain (from NO_x) and formation of ground level ozone (from the combination of HC and NO_x) [4]. The presence of CO and HC is due to incomplete combustion, whereas NO_x is mainly formed from the nitrogen in the air at the high temperatures inside the engine [3].

Also emitted is particulate matter (PM) with a wide range of properties. Particulate matter emissions from heavy duty diesel engines are a significant source of small (< 2.5 μm) particles in urban areas, and epidemiology has demonstrated that susceptible individuals are being harmed by ambient particulate matter [5]. It is estimated that one hundred thousand people die prematurely every year in Europe alone due to anthropogenic particulate matter [6], and fine small particles are now generally recognized as the main threat to human health from air pollution [7].

In addition, carbon dioxide (CO_2), which is also emitted, is a greenhouse gas, and it has been concluded that CO_2-emissions caused by man contribute to global warming [8].

In conventional stoichiometric gasoline engines, the three-way catalyst (TWC) can be used to oxidize CO and HC and reduce NO_x simultaneously. However, CO_2 cannot be converted over this catalyst - in fact, CO_2 is among

the final products of any complete CO and HC oxidation. If emissions of CO_2 are to be reduced, there must instead be a change of fuel, an increase in fuel efficiency and/or an overall change of engine technology (e.g. from combustion engine to fuel cell or electrical battery).

While facing all these problems, the transport demand in Europe is still increasing [1]. A necessary increase in fuel efficiency can be brought about by a shift from stoichiometric engines to *lean-burn* engines (such as the diesel engine), where there is an excess of air present at combustion. This however also means that there will be an excess of oxygen present in the exhaust gases in the aftertreatment system, which renders the TWC unusable, as it can no longer oxidize CO and HC and reduce NO_x at the same time in the oxidizing environment. New aftertreatment systems must therefore be designed for the lean-burn engines.

Particles are present in several forms in lean-burn exhaust gas aftertreatment systems. To begin with, the application of certain NO_x-reduction technologies introduces droplets from a spray into the diesel exhaust gas as a step in the emission abatement process. In addition, particulate matter is formed during combustion. These particles start to grow from tiny carboneous structures or condensed volatiles and eventually form larger porous agglomerates. One wishes to remove these particles from the exhaust. As legislation changes towards also regulating the number of particles emitted [9], gasoline engines might need such devices as well [10].

The continuous increase of available computational resources has shifted much of the engineers' focus from the time-consuming and expensive construction of pilot-scale prototypes towards simulation-driven development of new aftertreatment solutions. Not only are there huge savings to be made on cutting the design and development time [11, 12], but computational simulations can often provide more information than what is available from traditional experimental techniques. For example, the use of computational fluid dynamics (CFD) may provide access to the entire flow field of a chemical reactor at any given time, something which is typically impossible to obtain from experiments. It is today generally accepted that the continued development of lean exhaust gas aftertreatment systems will be driven by modeling and simulations [13, 14].

In an effort to come up with new, better and/or optimized designs of the various devices in an aftertreatment system, computer-aided simulations are thus indispensable. The work presented in this thesis discusses and assesses CFD-based modeling of the momentum, heat and mass transfer and the chemical reactions of various types of particulate flows in typical aftertreatment systems.

1.2 Objectives of the thesis

The objectives of this thesis are:

- To provide a detailed analysis of the range of phenomena that affect the motion and deposition of diesel and gasoline particulate matter and urea-spray droplets in an exhaust gas aftertreatment system.
- To derive computationally efficient models for numerical simulations of particle motion and estimations of the particle trapping efficiency in exhaust gas aftertreatment system devices, such as the channels or the porous walls of a monolithic reactor.
- To use detailed numerical simulations as a means of evaluating novel ways to deal with automotive pollution control, for example by proposing new reactor designs or modes of reactor operation.

1.3 Organization of the thesis

This thesis is organized as follows: First, the different types of particles and devices in a generic aftertreatment system are introduced. After that, there is a theoretical introduction to the field, which concludes with an account of previous works related to particulate flows in aftertreatment systems. The contents of the included papers are then summarized in a succeeding section. The aim is to clearly and efficiently connect each study to its physical application in the real-world system, and to give a sufficient theoretical background to the fluid dynamics aspects of the studied subsystem. The thesis finally concludes with a discussion, a summary of the work and an outlook on the future work.

Chapter 2

The exhaust gas aftertreatment system

2.1 Introduction

One of the biggest engineering challenges with problems related to exhaust gas aftertreatment systems is that such problems typically span a wide range of spatial scales [15]. As an example, the various spatial scales involved in diesel particulate matter filtration are illustrated in Figure 2.1. To be able to discuss the modeling and simulation of particulate flows on these different length and time scales, the characteristic properties of the particles and the devices must be known. It is therefore the aim of this chapter to first introduce the particles in a generic aftertreatment system (i.e. soot particles and droplets), and then the different devices that constitute the system.

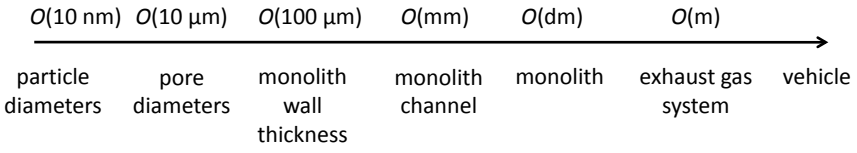

Figure 2.1: Illustration of the wide range of spatial scales involved in diesel particulate matter control.

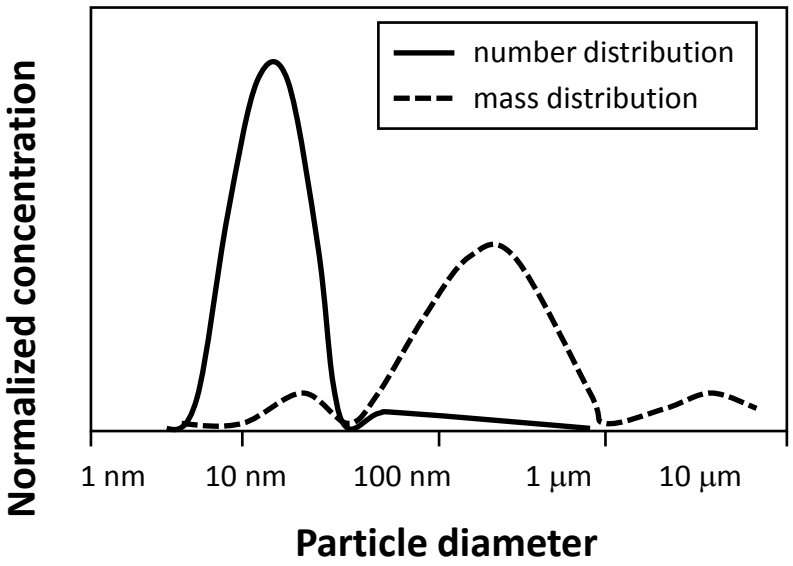

Figure 2.2: Illustration of the size distribution of diesel particulate matter [cf. 10].

2.2 Particles

2.2.1 Particulate matter (PM)

In contrast to the gaseous pollutants from internal combustion engines, particulate matter is not at all well defined. In fact, the most common definition of the term particulate matter contains everything that is collected on a filter paper in exhaust that has been diluted and cooled to 52°C [16]. Therefore, the constituents of diesel particulate matter include a wide range of chemical species and both a solid fraction (carbonaceous materials and ash) and a liquid fraction (condensed hydrocarbons, water and sulfuric acid) [17]. An illustration of the size distribution of diesel particulate matter is provided in Figure 2.2.

The smallest, primary particles - denoted the *nuclei mode* particles - are formed already at combustion in the engine cylinder. They increase in number as the exhaust gas passes through the aftertreatment system via a number of different nucleation mechanisms (including condensation of volatile substances from the gas phase). These nuclei mode particles are a few nanometers in size when they first appear and they thereafter grow [18]. There is a peak in the number concentration at about 10 - 20 nm. Since these particles are formed from condensed liquid material or tiny carbonaceous fragments, they are more or less spherical [19].

As vapors condense or gases adsorb onto the nuclei particles, they may

become 'sticky' and collision with other particles causes agglomeration. This process produces a second type of particulate matter known as *accumulation mode* particles. These particles typically have a core of primary carbon fragments and/or ash from the lubricating oil, over which hydrocarbons and sulfur species condense or adsorb. The accumulation mode particles have a peak in the number concentration at sizes around 100 - 200 nm, and since they are formed from agglomeration processes, they are not as spherical as the smaller particles [19, 20]. Whereas most of the particles in diesel exhaust are nuclei mode particles, the largest portion of the mass is located among accumulation mode particles.

Finally, there is a type of particles referred to as the *coarse mode* particles. These are very large agglomerates of sizes in the micrometer range, which are not formed due to the combustion but from the interaction between accumulation mode particles as they deposit and re-entrain from surfaces in the aftertreatment system [10]. On a number basis, these particles are insignificant, but a non-negligible part of the total mass of particulate matter may be present in this form.

The composition and sizes of particulate matter in an aftertreatment system are complex functions of the fuel, the engine characteristics and operation, and the aftertreatment system itself [20]. Gasoline particulate matter, for example, is similar to diesel particulate matter with the exception that the total mass of particulate matter emitted is lower and that the nuclei mode particles are generally dominating [10]. The usage of ultra low sulfur diesel has been shown to significantly decrease the formation of nuclei mode particles [21], which highlights the role of sulfur-containing species in the nucleation of particulate matter [cf. e.g. 22]. In addition, biodiesels - which contain more oxygen than conventional diesel - may suppress the formation of agglomeration mode particles [21, 23]. Furthermore, exhaust gas recirculation[1] (EGR) is known to increase the emissions of particulate matter [24], and fouling of EGR coolers by particulate matter can be a problem in diesel engines [25].

Because of the complex interplay between the engine, the aftertreatment system components and the fuel, it is extremely difficult to investigate the effect of any of these factors on the particulate matter emissions individually [20]. In fact, it has proven itself difficult to even find standardized ways of measuring the particulate matter emissions [26].

For the optimization of next generation's diesel vehicles to be successful, the entire exhaust line must be taken into account in the optimization

[1] EGR is a common method to reduce the engine-out levels of NO_x (due to lower flame temperature and oxygen concentration).

process. Research on the dynamics of the flow of particulate matter in the aftertreatment system is of utmost importance for that work to be prosperous.

2.2.2 Droplets

Since there is an excess of oxygen in the diesel exhaust, NO and NO_2 cannot be reduced to N_2 without a reductant being present. Several technologies exist that address this problem: urea-SCR, HC-SCR and NO_x-traps [27]. The selective catalytic reduction (SCR) technologies rely on the dosing of a reducing agent to the exhaust gas flow upstream the SCR catalyst. The reducing agent may be either urea dissolved in water (as in urea-SCR) or the fuel itself (as in HC-SCR). In either case, the reducing agent is in liquid form and a spray is used to enhance the evaporation (and in the urea case, also the decomposition of urea into ammonia). The use of an SCR catalyst is therefore intimately linked to the introduction of droplets into the exhaust gas flow.

The solution that is sprayed into the exhaust gases in urea-SCR consists of 32.5% urea in water (by weight). At the spray nozzle, the liquid is injected under high pressure, forming sheets that continually break up due to various disturbances (e.g. interaction with the nozzle geometry and the exhaust gas) [28]. This primary breakup creates liquid fragments and large droplets which undergo secondary breakup to form the fine droplets of the spray. These final droplets are initially on the order of 100 μm in diameter. Due to the evaporation of water and the subsequent decomposition of urea, there is a continuous transport of mass from the droplets which diminishes their diameter with time.

The aim of the urea-spray is to supply ammonia to the SCR-catalyst for the reduction of NO_x to nitrogen. However, the chemistry of urea is complex and several other chemical species can be produced in the aftertreatment system [29, 30]. The formation of deposits of urea or urea decomposition products in the aftertreatment system is now a well-known problem with the urea-SCR system [29, 31–38]. It has been suggested that the deposit formation could be the result of a poorly adjusted spray [29, 31].

In addition, the ammonia distribution over the inlet cross-section of the SCR-catalyst should preferably be even, so as to avoid ammonia slip or insufficient NO_x-reduction. To this end, the introduction of static mixers has also been suggested [39, 40].

The development of highly accurate urea-spray models will be necessary to make efficient optimization of the urea-SCR system possible. An integral part of this challenge is a proper description of the flow dynamics of the

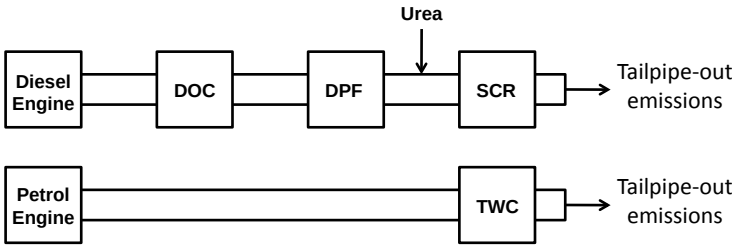

Figure 2.3: Illustrations of a generic diesel aftertreatment system with urea-SCR (above) and a generic gasoline aftertreatment system (below).

urea-spray.

2.3 The aftertreatment system devices

The design of an exhaust gas aftertreatment system varies considerably depending on a number of factors (e.g. the manufacturer, the size of the vehicle, the capacity of the engine and the legislation in the country of intended use). Figure 2.3 illustrates two generic aftertreatment systems, one for a diesel engine (with urea-SCR) and one for a petrol engine. The components that will be discussed in this chapter are the diesel oxidation catalyst (DOC), the wall-flow (DPF) or flow-through (FTF) particulate filters, and the selective catalytic reduction (SCR) catalyst. The focus will be on the relation of each component to the types of particulate flow expected in connection to it. Finally, the three-way catalyst (TWC) used in gasoline applications will also be mentioned in relation to its diesel applications counterparts. However, since most of these components are merely variations of one fundamental type of chemical reactor, the description of these devices will start with a description of *the monolithic reactor*.

2.4 The monolithic reactor

Monolithic reactors are today the industrial standard for automotive pollution control applications. A monolithic catalyst reactor is typically made out of a porous material (such as cordierite or silicon carbide) which constitutes the substrate that forms the basic shape of the reactor. This substrate can also be metallic. A typical ceramic substrate design is illustrated in Figure 2.4. The exhaust gas flows through a large number of parallel axial channels. A second layer of porous material, the so-called washcoat, is deposited inside the monolith channels. The purpose of the washcoat is to maximize the

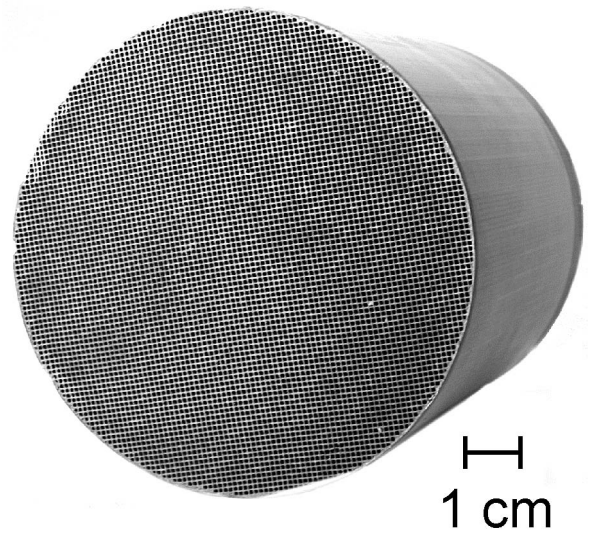

Figure 2.4: An example of a monolithic reactor for automotive pollution control. The gas flows through thousands of parallel channels where the catalytic material has been deposited on the internal walls.

available surface area onto which the catalytic material finally is deposited. The inlet to four monolith channels is schematically depicted in Figure 2.5.

The reactions in a monolithic reactor typically involve three different steps: mixing of the phases that are being transported through the channels (e.g. gas and particles or droplets), mass transfer to and from the channel walls, and the chemical reactions occurring on the surface of the solid catalyst dispersed within the washcoat [41]. In general, the interaction between the different transport processes and the chemical reactions is intricate and complicates the modeling of the performance of the monolithic catalyst reactor.

The monolithic reactor is said to operate within a certain *regime*, depending on the (local) temperature [42, 43]. For low temperatures, the overall reaction is controlled by the reaction kinetics. As the temperature increases, the pore diffusion inside the washcoat may affect the reaction. At higher temperatures (typically from 250-300°C and up), the rate of reaction is limited by the mass transfer between the gas and the monolith walls. The transition from kinetic control to mass transfer control is referred to as catalyst *light-off*.

Since the flow in a standard monolithic channel is laminar, the reacting species are brought to the wall by molecular diffusion [42]. The reactor performance in the mass transfer controlled regime is therefore a strong function

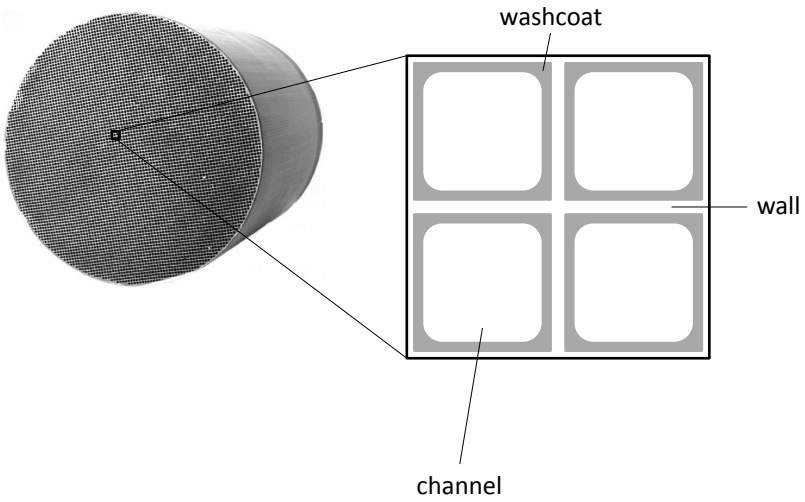

Figure 2.5: Illustration of the entrance to four monolith channels. The channels of the substrate have square cross-sections, which are rounded by the washcoat as it is deposited onto the channel walls. For approximate spatial scales, see Figure 2.1.

of the gas flow field inside the channels. On the contrary, the light-off temperature is generally mostly dependent on the reaction kinetics, and thus on the choice of catalyst/washcoat-system [43].

2.5 Diesel oxidation catalyst (DOC)

The diesel oxidation catalyst is a monolithic reactor whose purpose is to effectively oxidize gaseous pollutants. In this way, the typical products of incomplete combustion - carbon monoxide (CO) and various hydrocarbons (HC) - are converted into the final products carbon dioxide (CO_2) and water (H_2O).

Also the soluble organic fraction of diesel particulate matter entering the diesel oxidation catalyst will be oxidized to CO_2 and H_2O. On the other hand, the sulfur content of the exhaust gases - entering the DOC as gaseous SO_2 - will too be oxidized, leading to the formation of sulfate nuclei mode particles [22, 44]. It is therefore not uncommon that the number count of diesel particulate matter *increases* after the passage through the DOC.

In addition to oxidizing CO and HC, the DOC also oxidizes nitric oxide (NO) to nitrogen dioxide (NO_2). Before the exhaust is let out into the ambient air, the total NO_x level must be reduced significantly. The NO_2-production is however beneficial, as NO_2 is typically used in a downstream soot filter to oxidize the trapped particulate matter at much lower temperatures than what can be achieved with oxygen [45]. It may also be beneficial

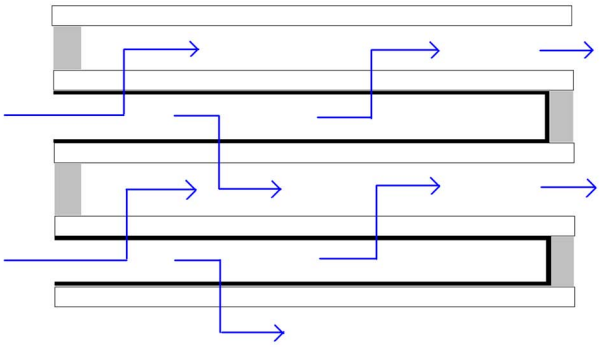

Figure 2.6: Schematic illustration of the standard DPF design. The channels are plugged in either end (grey), forcing the gas to flow through the walls (arrows) and the soot (black) is deposited along the inlet channels.

for the SCR catalyst, as the typical NO_x content in diesel exhaust is to 95% NO [45] and the SCR conversion rate has a maximum for a 1:1 stoichiometric mixture of NO and NO_2 [46].

2.6 Wall-flow diesel particulate filter (DPF)

Since the diffusion of particulate matter to the catalytically active walls of the standard monolithic reactor is very slow and ineffective, the monolithic reactor has not been successful at reducing the particulate matter content in its original design [cf. 47]. The wall-flow diesel particulate filter (DPF) is instead the most commonly used reactor for removal of particulate matter in diesel applications.

In the DPF, every channel in the ceramic monolithic reactor is plugged in either end, creating a chessboard-like appearance of the monolith front and back [48]. The exhaust gas is therefore only allowed to enter the channels which are open towards the inlet side, the so-called *inlet channels*. The gas is then forced to flow through the porous wall into the four adjacent *outlet channels*. Once the DPF has accumulated particles inside and on the porous walls of the inlet channels, the trapping efficiency goes up to over 90% [49]. Not all DPF designs include catalytically active material, but it is believed that catalyzed DPFs will be necessary to comply with the forthcoming years' updated emission legislation [50, 51]. In Figure 2.6, the standard DPF design is illustrated.

The main drawbacks with the wall-flow design are that the pressure drop over the DPF is excessive (more than an order of magnitude larger than over the DOC) [49] and that there are several problems associated with regen-

erating the filter [52]. At low exhaust gas temperatures, the oxidation of particulate matter (passive regeneration) is not necessarily fast enough to balance the accumulation by trapping. The filter is said to be actively regenerated when the exhaust gas temperature is artificially increased for a short period of time (e.g. by post-combustion fuel injection) to start the oxidation reaction. As the oxidation reaction is highly exothermic, the temperature of the filter will rise quickly and most of the soot will burn off. However, the temperature gradients may cause serious mechanical damage to the DPF or a downstream SCR catalyst. Besides, after regeneration there will always be some unburned soot and ash still left in the filter, increasing the risk that the filter will eventually clog or malfunction as it is being aged. In an investigation of a DPF from a passenger car, it was for example found that after approximately 120,000 km, more than 50% of the filter volume was filled with ash [53]. One may therefore conclude that the wall-flow filter solves the problem of trapping enough diesel particulate matter, but at the expense of introducing a high fuel penalty and a serious risk when it comes to the robustness of the aftertreatment system. For applications where one does not need more than 90% trapping efficiency, such as in light-duty or gasoline applications, a different solution - e.g. a flow-through filter - would therefore be preferred.

2.7 Flow-through particulate filter (FTF)

A flow-through filter (FTF) is a monolithic reactor that is designed in such a way that the trapped particulate matter is never allowed to totally block the fluid flow[2]. The aim is to obtain a reduction of the particulate matter content by oxidation with NO_2 generated in an upstream conventional DOC or in the flow-through filter itself. The trapping efficiency is generally significantly lower than in a DPF but much higher than in a traditional DOC. As a result, the flow-through filter is a much more robust device than the wall-flow filter. The alternate design is usually a variant of the monolithic reactor with e.g. protrusions, porous parts or obstacles [54]. Flow-through filters are therefore often manufactured from metallic substrates, since these are easy to shape, bend and fold [48]. Depending on the specific design, the flow-through filter may target either small, large or intermediate sizes.

The other types of flow-through filters (not discussed further in the cur-

[2]The term flow-through filter is sometimes used ambiguously. In the current work, the most common interpretation of the flow-through concept will be used: a DOC with an alternate design which allows trapping of particulate matter, or at least prolonged retention times of particulate matter within the device.

rent work) include those made entirely out of ceramic or metallic foams, metal fleece or a wiremesh [48, 55–58]. Such filters may exhibit high filtration efficiencies, but at the price of an increase in pressure drop and reduced robustness. For a further discussion on such filters, see [52].

2.8 Selective catalytic reduction (SCR) catalyst

Selective catalytic reduction (SCR) is one of several technologies available for NO_x-reduction in lean exhaust [27]. In the current work, the discussion is confined to urea-SCR, which is probably the most viable solution in commercial use today [31].

In urea-SCR, the reduction of NO and NO_2 to N_2 takes place over a dedicated SCR catalyst with ammonia as the reducing agent. The ammonia is produced from the decomposition of urea, which is introduced dissolved in an aqueous spray (the so-called *urea-spray*).

The aim with the urea-spray in the urea-SCR system is that the droplets created by the spray should be totally evaporated/decomposed before they reach the SCR reactor inlet side. The distribution of the reducing agent should also be uniform over the inlet, or insufficient NO_x-reduction and ammonia *slip* may result. The latter is a term used to denote when the SCR process malfunctions (due to inadequate dosing and/or distribution of the reducing agent) and the reducing agent is released to the ambient air.

2.9 Three-way catalyst (TWC)

Since the air-to-fuel ratio in gasoline applications is equal to the stoichiometric ratio, there is no oxygen excess in gasoline exhaust. The three-way catalyst (TWC) is therefore the gasoline counterpart of a combined DOC and SCR catalyst, where both oxidation and reduction of HC, CO and NO_x, respectively, can take place at the same time. From the perspective of modeling particulate flows, the three-way catalyst is therefore essentially identical to the DOC in diesel applications.

Chapter 3

Particulate flow

3.1 Introduction

Particles in aftertreatment systems can be divided into two main groups: solid and fluid particles[1]. Whereas solid particles often can be assumed to be rigid and of arbitrary shape, fluid particles strive for a spherical shape due to surface tension forces, while they might distort significantly due to external influence. The modeling of droplet motion and soot particle motion therefore differ on some critical points. This chapter aims at describing the fundamentals of particle transport and deposition. As most of the current work has been done for solid particles, this theoretical background will also focus on solid particles. Unless otherwise noted, the particles will also be assumed to be spherical.

3.2 Particle transport parameters

There are three parameters that are fundamental to any discussion about the transport of particles by fluid flow. The first of these is the particle Reynolds number:

$$Re_p = \rho d_p U_r / \mu \tag{3.1}$$

The particle Reynolds number characterizes the flow around a particle. Because of the small sizes of diesel soot particles and their low relative velocities to the exhaust gas, their particle Reynolds numbers rarely exceed unity. The flow around the particles is then in the so-called *creeping flow* regime, where viscous forces predominate. The flow pattern is almost symmetric,

[1]The term 'fluid particle' is here used to denote a particle which is not composed of solid matter but of a fluid, in line with the terminology defined by Clift et al. [59].

the flow adheres to the particles, and the wake is free from oscillations. For droplets in a urea-spray, on the other hand, both the sizes and the relative velocities are larger. This shifts the particle Reynolds number to higher values (generally starting about 200 at injection and from there decreasing due to evaporation and adaptation to the gas flow velocity). Physically, this is reflected in the appearance of small eddies at the rear stagnation point of the flow around the droplet. These eddies might grow in size and separate from the droplet. This change in flow characteristics has a profound effect on the heat and mass transport to and from the droplets, but also aggravate the possibilities to obtain analytical solutions to the equations of motion of the droplets, as will be discussed later.

Another important parameter in particulate flow that characterizes the inertia carried by a particle is the particle response time (also known as the particle relaxation time):

$$\tau_p = \frac{\rho_p d_p^2 C_c}{18\mu} \tag{3.2}$$

The particle response time is by definition the time it takes for the particle velocity to be accelerated to 63.2% of that of the fluid, if the particle is initially at rest and there is a step change in the fluid velocity. The ratio of the particle response time to a characteristic time scale of the system will then characterize the tendency of the particle to follow the fluid motion. This ratio is a dimensionless number known as the Stokes number:

$$St = \tau_p/\tau_s \tag{3.3}$$

When the Stokes number is small, particle motion is dominated by the gas phase motion, and the particles tend to follow the fluid streamlines. For large Stokes numbers, the particle inertia is dominating the particle behavior, and the particle has a tendency not to respond to fluctuations in the fluid velocity. The fluid-particle interaction at intermediate Stokes numbers is such that the particle may be 'flung out' of fluid motions (e.g. turbulent eddies).

For soot particles, the particle response times are usually much smaller than the typical system response times. The urea-spray droplets are larger and may have Stokes numbers close to or above unity, in which case they move more independent of the fluid motion. However, as the droplet size decreases due to evaporation and decomposition, the droplets start to follow the fluid motion more and more closely. Thus, a detailed resolution of the gas phase flow field is necessary in both cases in order to correctly describe particle motion within a system.

3.3 The fluid flow field

3.3.1 The continuum concept

A fluid is by definition a substance that deforms continuously under the action of a shear stress. The two most common types of fluids are liquids and gases, but in the current work the discussion is limited to gases. Furthermore, it is assumed that the flow is incompressible[2].

A fluid is typically composed of a vast number of molecules. There are for example more than 10^{25} molecules in one cubic meter of air at room temperature and atmospheric pressure. It is therefore not realistic to predict the individual motion of all the molecules contained in a typical industrial application. However, if the smallest volume of interest in an analysis still contains a sufficient number of molecules, it is possible to obtain meaningful statistical averages. The molecules are then treated as continuous distribution of matter, i.e. as a *continuum*.

Whether the continuum assumption is valid or not can be judged from the Knudsen number:

$$Kn = \lambda / L \tag{3.4}$$

where L is a characteristic length scale and λ is the mean free path of the gas[3]. When the Knudsen number is larger than 0.015, the basic assumptions underlying continuum theory are violated [62].

The smallest particles that constitute particulate matter are smaller than the mean free path of the exhaust gas. In exhaust gas aftertreatment system applications, continuum theory does therefore not hold for the flow around these particles. It is also not valid for the flow inside the pores of the washcoat or inside the porous walls of the monolith substrate.

3.3.2 The Navier-Stokes equations

In order to obtain the spatial and temporal variation of a fluid flow field in a given system, one must solve the differential equations that determine the fluid motion. These are derived from two fundamental principles: the conservation of mass and Newton's second law of motion. The law of conservation of mass states that mass cannot be created or destroyed, and reads

[2] An interesting investigation of compressibility effects in diesel particulate matter filtration is provided by Torregrosa et al. [60].

[3] The mean free path can be calculated according to Maxwell [61], and is approximately 100 - 200 nm for typical exhaust gas conditions.

in differential form for an incompressible fluid:

$$\frac{\partial u_i}{\partial x_i} = 0 \tag{3.5}$$

Equation (3.5) is usually referred to as the continuity equation.

Newton's second law of motion for a fluid control volume states that the time rate of change of momentum within the control volume is given by the sum of the external forces acting on the control volume minus the net rate of momentum efflux. In differential form, the momentum balances for a Newtonian fluid[4] in the three coordinate directions are referred to as the Navier-Stokes equations [63, 64]:

$$\rho\left(\frac{\partial u_i}{\partial t} + u_j\frac{\partial u_i}{\partial x_j}\right) = -\frac{\partial p}{\partial x_i} + \frac{\partial}{\partial x_j}\left(\mu\frac{\partial u_i}{\partial x_j}\right) + \rho g_i \tag{3.6}$$

Two fundamental fluid properties appear in these equations: the density (ρ), which is defined as the mass per unit volume, and the viscosity (μ), which is a measure of the fluid resistance to the rate of deformation when acted upon by shear forces.

The fluid layer in the closest proximity to a boundary is assumed to have zero relative velocity to the boundary, which is referred to as the *no-slip* boundary condition. It has been observed experimentally that the flow fields obtained from the Navier-Stokes equations with this boundary condition closely match the experimental data [65]. However, it is always possible to find a small volume very close to a boundary in which there are not enough molecules to obtain meaningful statistical averages and continuum theory breaks down. In other words, within a distance of approximately one mean free path from the boundary, the Navier-Stokes equations do not hold. Consequently, when the mean free path is significant to the size of the overall geometry, the Navier-Stokes equations will cease to be valid throughout the entire domain.

An important simplification of the Navier-Stokes equations can made when the inertial forces are negligible in comparison to the viscous forces[5]. In this situation, the convective terms on left hand side of equation (3.6) can be neglected and the problem becomes linear. This is the type of flow denoted creeping flow or *Stokes flow*.

[4] A Newtonian fluid is a fluid that obeys Newton's law of viscosity, according to which the shear stress is proportional to the rate of shear strain, the constant of proportionality being the fluid viscosity.

[5] That is, when the flow Reynolds number ($Re = \rho LU/\mu$) is much smaller than unity.

3.3.3 Computational fluid dynamics (CFD)

Solving equations (3.5) and (3.6) with the appropriate boundary and initial conditions provides access to the entire velocity and pressure field in a given domain. Unfortunately, the Navier-Stokes equations are non-linear partial differential equations, and analytical solutions are only available for the simplest of cases. For almost any situation of practical interest, the only way to obtain the flow field is by experimental observation or by numerical solutions (i.e. *numerical simulations*). Such simulations are typically performed using a computational fluid dynamics (CFD) technique.

In a CFD approach, the geometry of interest is first defined and then discretized into discrete computational cells. Thereafter, the equations governing the flow field must also be discretized. In the current work, the well-established finite-volume method has been employed for this purpose.

Within the finite-volume framework, the partial differential equations are evaluated as algebraic equations. This can be done as the discretization of the integrated governing equations of fluid flow over all the control volumes in the solution domain involves the substitution of finite-difference-type approximations for the terms in the integrated equation, which converts the integral equations into a system of algebraic equations [66]. Because of the complexity and non-linearity of the problem, the solution approach is iterative.

CFD simulations are extremely powerful in that they can provide access to the entire flow, temperature and species concentrations fields in the computational domain of interest[6].

3.3.4 Turbulence modeling

Complete information about fluid flows in the continuum limit is believed to be available from the solutions to equations (3.5) and (3.6) with the appropriate boundary conditions. Solving these equations directly introduces no error other than that of the numerical methods used and is called direct numerical simulation (DNS). However, the computational cost of solving these equations can become overwhelming, as it approximately proportional to the cube of the flow Reynolds number [67]. For problems of industrial scale, approximations typically have to be introduced in order for a solution to be obtainable. The process in which the original Navier-Stokes equations are

[6]When temperature and species concentrations are also of interest, additional balance equations for energy and continuity of the involved species are solved together with equations (3.5) and (3.6).

altered in order to decrease the computational cost is commonly referred to as *turbulence modeling*.

In the current work, two turbulence modeling approaches have been used where the full Navier-Stokes equations could not be solved directly. These approaches are the large eddy simulation (LES) approach and the Reynolds-averaged Navier-Stokes (RANS) approach.

Large eddy simulation approach (LES)

The idea behind LES is to filter the Navier-Stokes equations. In many finite-volume implementations, such as the one used in the current work, the computational mesh acts as the filter. Spatial scales smaller than the grid spacing are therefore not resolved, but their effect on the resolved scales can be taken into account via a subgrid-scale model[7]. The filtered, incompressible continuity equation and Navier-Stokes equations for the resolved field are:

$$\frac{\partial \overline{u}_i}{\partial x_i} = 0 \tag{3.7}$$

$$\rho \left(\frac{\partial \overline{u}_i}{\partial t} + \frac{\partial \left(\overline{u}_i \overline{u}_j \right)}{\partial x_j} \right) = -\frac{\partial \overline{p}}{\partial x_i} + \frac{\partial}{\partial x_j} \left(\left[\mu + \mu_t \right] \frac{\partial \overline{u}_i}{\partial x_j} \right) + \rho g_i \tag{3.8}$$

The rationale behind LES is that the large scales are most geometry-dependent (and therefore most problem-dependent), whereas the smaller scales are believed to be more isotropic and therefore easier to model. However, there are a number of open questions regarding the conceptual foundation of LES [70], e.g. the dependence of the results on the filter width and the relations between the statistics of the resolved velocity field, the filtered velocity field and the physical velocity field.

Although LES may substantially decrease the computational cost of solving for the fluid flow field compared to DNS, it is still computationally very expensive. In addition, since whenever a three-dimensional and transient flow field is realized, any mean results must be obtained from averaging, long simulation times are typically necessary. Therefore, LES is limited to relatively small geometries.

Reynolds-averaged Navier-Stokes approach (RANS)

A different approach to obtaining the mean flow field from the Navier-Stokes equations is to solve for it directly. This is the idea behind the RANS approach. First, the instantaneous variables are split into a mean component

[7] In the current work, whenever LES is performed, the dynamic subgrid-scale model of Germano et al. [68] and Lilly [69] is used.

and a fluctuating component (the so-called Reynolds decomposition):

$$u_i = U_i + u_i' \tag{3.9}$$

$$p = P + p' \tag{3.10}$$

The instantaneous variables in the Navier-Stokes equations are then substituted for the decompositions. By time-averaging the substituted Navier-Stokes equations on a time-scale longer than that of the turbulent fluctuations but shorter than that of any variations in the mean flow, the RANS equations are obtained. However, this procedure produces a term, known as the Reynolds stresses ($-\rho\langle u_i' u_j' \rangle$), that accounts for the coupling between the mean (resolved) and the fluctuating (unresolved) part of the velocity field. The Reynolds stresses are therefore unknown and have to be modeled, and several approaches exist. One of the most often used involves modeling the Reynolds stresses as being proportional to the gradient of the mean velocity in an analogy with the viscous stresses. The Reynolds stresses can then be computed using a turbulent viscosity, μ_t. The incompressible RANS equations finally become:

$$\frac{\partial U_i}{\partial x_i} = 0 \tag{3.11}$$

$$\rho\left(\frac{\partial U_i}{\partial t} + U_j \frac{\partial U_i}{\partial x_j}\right) = -\frac{\partial p}{\partial x_i} + \frac{\partial}{\partial x_j}\left[(\mu + \mu_t)\frac{\partial U_i}{\partial x_j}\right] - \frac{2\rho}{3}\frac{\partial k}{\partial x_i} \tag{3.12}$$

In the current work, the turbulent viscosity is determined using a turbulence model in which two additional transport equations are solved: one for the turbulent kinetic energy ($k = \frac{1}{2}\langle u_i' u_i' \rangle$) and one for either the turbulent dissipation rate (ε) or the specific dissipation rate (ω) [cf. 71].

There is a huge reduction in the computational load associated with solving a problem when using RANS instead of LES or DNS. However, this undeniable advantage comes at a great price. Most RANS models cannot accurately predict neither the mean flow in a non-circular cross-section [72] nor accurate profiles of turbulent fluctuations [73] - facts which strongly suggest that RANS models should be avoided whenever possible for simulations of particle dispersion and deposition.

3.4 The forces on a particle

3.4.1 The aerodynamic force on a particle in isothermal flow

The total aerodynamic force on a spherical particle submerged in a fluid flow field is obtained by integration of the pressure and viscous forces over the

particle surface. The net action of these forces will determine the particle motion, according to Newton's second law of motion:

$$\frac{dx_{p,i}}{dt} = u_{p,i} \tag{3.13}$$

$$m_p \frac{du_{p,i}}{dt} = m_p g_i + \oint_s \left[-p\delta_{ij} + \mu \left(\frac{\partial u_i}{\partial x_j} + \frac{\partial u_j}{\partial x_i} \right) \right] n_j dS \tag{3.14}$$

In a *multiphase DNS* method, the actual flow field is resolved around the particle and the particle motion may be determined directly from equations (3.13) and (3.14). However, such methods are only generally computationally affordable when there are relatively few particles present in the system.

In a situation where there are many particles present, but the particle size is small compared to the containing geometry and the particle loading is low, *Lagrangian particle tracking* is a viable alternative. In this approach, the flow field around each particle is not resolved explicitly. This means that the second term on the right hand side of equation (3.14) has to be estimated from average quantities in the computational cell that the particle is currently in.

Maxey & Riley [74] derived the particle equation of motion for a small rigid sphere in nonuniform, isothermal flow in the limit of zero particle Reynolds number:

$$\begin{aligned} m_p \frac{du_{p,i}}{dt} = {} & (m_p - m_f) g_i + m_f \frac{Du_i}{Dt} \\ & - \frac{1}{2} m_f \frac{d}{dt} \left(u_{p,i} - u_i - \frac{1}{40} d_p^2 \nabla^2 u_i \right) \\ & - 3\pi d_p \mu \left(u_{p,i} - u_i - \frac{1}{24} d_p^2 \nabla^2 u_i \right) \\ & - \frac{3}{2} \pi d_p^2 \mu \int_0^t \left(\frac{\frac{d}{d\tau} \left[u_{p,i}(\tau) - u_i(\tau) - \frac{1}{24} d_p^2 \nabla^2 u_i(\tau) \right]}{\left[\frac{\pi\mu}{\rho} (t - \tau) \right]^{1/2}} \right) d\tau \end{aligned} \tag{3.15}$$

The different contributions on the right hand side of equation (3.15) are usually referred to as individual forces acting on the particle. The physical interpretation of these terms are then, from left to right, that they represent the effects of buoyancy, pressure gradient of the undisturbed flow, added mass, viscous Stokes drag, and the augmented drag from the history term[8]. The terms involving $\nabla^2 u_i$ are the Faxén corrections.

[8]Differently put, the Stokes drag is the steady aerodynamic force on a sphere in uniform Stokes flow ($F = 3\pi\mu d_p (u_i - u_{p,i})$), and the added mass and history forces are the unsteady contributions to this drag force.

It is often possible to neglect several of these contributions to the net force, which also typically reduces the computational cost of solving for the particle motion. For a more detailed discussion on the various forces and their interpretation, see e.g. [59, 74–76].

Since the work of Maxey & Riley is based on the assumption of a low particle Reynolds number, their results are not applicable to urea-spray droplets. Unfortunately, because of the non-linearities inherent in the Navier-Stokes equations at finite Reynolds numbers, the attempts at obtaining expressions for the different forces acting on particles under such conditions have mainly resulted in empirical models. Some of these models, relevant for the urea-SCR application, are discussed in **paper I**.

Finally, if the particles of interest behave more or less entirely like molecules of the gas in which they are contained, their motion and dispersion can be modeled as a diffusion process [77]. This approach is only applicable to very small particles and is discussed in more detail in **paper III**.

3.4.2 Effects of rarefaction on the aerodynamic force

The discussion in the previous section relies on the condition that the continuum hypothesis is valid. However, when the particle diameter becomes comparable to the mean free path of the gas, this is no longer the case. The aerodynamic force on the particle can then not be determined from the solution to the Navier-Stokes equations. Although altering the boundary conditions has been a successful approach to extending the validity of the Navier-Stokes equations for duct flow into the rarefied regime, this approach has not been able to allow satisfactory predictions of the drag on a spherical particle [78]. Instead, corrections based on experimental data are usually relied upon.

Cunningham [79] found theoretically that the no-slip boundary condition is not appropriate for the flow of a rarefied gas around a small particle. He therefore modified the Stokes drag with a correction factor. This correction factor still bears his name. Independently, Millikan [80] also proposed such a correction from experimental data. Millikan's experiments form the basis for the correlations which are typically used today to compensate for the decreased momentum transfer to particles in the rarefied flow regime [81, 82].

The drag reduction is however not the most important effect on the motion of particles in rarefied flow. As the particles become comparable in size to the gas molecules, their motion becomes meandering, being influenced by the large number of collisions with surrounding molecules. This phenomenon is called *Brownian motion*, after the Scottish botanist Robert Brown who were among the first to observe it [83]. Einstein [84] later derived the diffusivity

coefficient that characterizes the Brownian motion.

However, since the Brownian motion is molecular to its nature, it is averaged out in the derivation of the Navier-Stokes equations, and there can be no source of Brownian motion in the aerodynamic force obtained from the solution to those equations. In a continuum framework, Brownian motion therefore has to be modeled, for example via the introduction of a fictitious Brownian force to the particle equation of motion [85]. Note that this approach to modeling Brownian motion converts the particle equation of motion from an ordinary differential equation to a stochastic differential equation, with the associated limitations in the choice of numerical solution methods [86].

In theory, rarefaction will influence all contributions to the aerodynamic force (i.e. all terms on the right hand side of equation (3.15)), but in practice, effects other than that on the drag are rarely taken into account. A further discussion on this issue is provided in **paper IV**, which is dedicated to the derivation of a novel method to simulate the motion of particles in rarefied flow in narrow geometries.

3.4.3 Additional forces on particles

The motion of a particle in a flow field is not necessarily determined only by the aerodynamic forces. When the flow is not isothermal, particles will be subjected to a thermophoretic force, which acts in the negative direction of the temperature gradient [87]. Under extreme conditions, such as vehicle cold-start, thermophoresis might be a significant particle transport mechanism [88]. It has also been suggested that filters could be design to specifically take advantage of the thermophoretic effect [89].

Other forces that can become important include electrostatic forces and van der Waals interactions. These forces originate from permanent or induced charges on the particles and nearby surfaces, and are typically very short-ranged [75]. For an introduction to van der Waals forces, see [90]. Electrostatic forces are generally considered to be insignificant in traditional diesel particulate filtration devices [88, 118], but can be enhanced and employed in application-tailored devices such as electrostatic precipitators [91].

3.5 Particle motion in the fluid flow field

3.5.1 Coupling between phases

The extent to which the particulate phase and the continuous phase influence each other is referred to as the degree of *coupling*.

If it is assumed that the particles are influenced by the gas phase, but not vice versa, and that there is no significant interaction among suspended particles, the degree of coupling is denoted *one-way*. It is generally held that the one-way coupling assumption is fully appropriate for investigations of particle-fluid interaction in the limit of small particles and dilute flow [92], e.g. for soot particles in the exhaust gas flow.

The droplets in the urea-spray, however, significantly affect both the gas flow field (typically close to the injector) and the temperature and composition of the gas (due to the heat and mass transfer occurring in the system). This situation is referred to as *two-way* coupling, since the gas influences the droplets and vice versa. In a two-way coupled model, droplet momentum, heat and mass transfer effects are fed back to the continuous phase, so that the two phases are solved for in a coupled manner.

Finally, close to collecting surfaces in filters, such as in or near the porous walls of a DPF, the typical distances between particles or between particles and bounding walls are small. In such a situation, the particles influence the motion of the gas phase and also each other's motion. This degree of coupling is called *four-way* coupling.

3.5.2 Particle transport and deposition

The flow regimes of interest in exhaust gas aftertreatment systems include both laminar and turbulent flow as well as transitional flow. Laminar flow requires the least computational resources in a DNS, and for laminar flow in a straight duct (e.g. a monolith channel), the transport of particles in the wall-normal direction is entirely governed by molecular diffusion[9]. Therefore, particle transport in turbulent flow is in general much more complex, and it is thus the focus of the following discussion. A schematic picture of the near-wall region and the particle transport and deposition phenomena in turbulent flows is given in Figure 3.1.

[9]This is only strictly true for isothermal flow when the channel cross-sectional area is constant and there are no external forces on the particles.

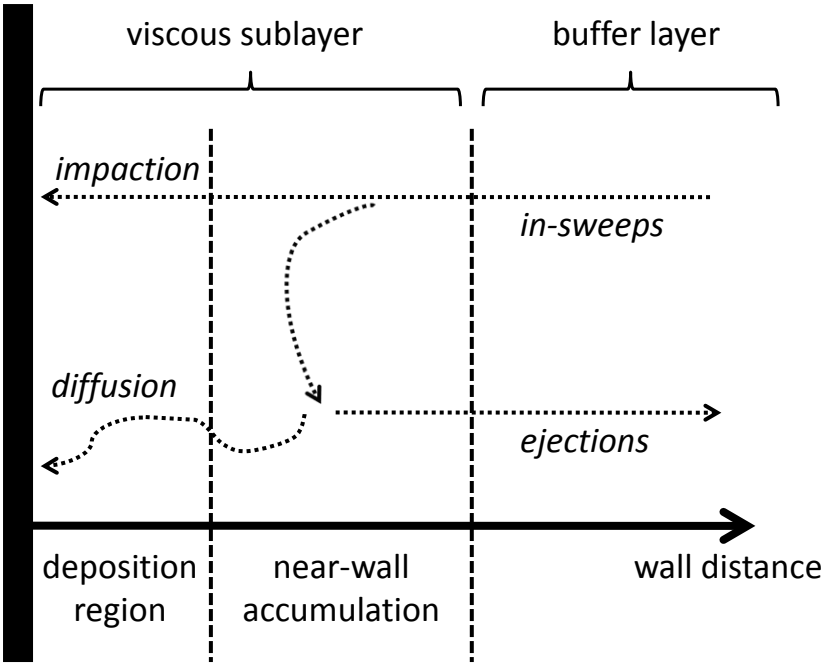

Figure 3.1: Conceptual illustration of the mechanisms responsible for near-wall particle accumulation and particle deposition in turbulent flows [cf. 92].

The deposition process

DNS of particle motion and deposition in turbulent flow fields have added much to the general understanding of particle deposition in turbulent flows [93–96]. McLaughlin [93] showed with DNS that aerosol particles, even if entering a turbulent channel flow with random initial locations and with initial velocities equal to that of the local fluid velocity, tend to accumulate in the viscous sublayer. If the particles possess enough inertia, they might deposit directly from outside the wall region. Such particles typically wander more or less parallel to the wall until they are trapped in a turbulent eddy in the so-called buffer region (cf. Figure 3.1), which then brings them directly to the wall [94]. Particles that are thrown into the near-wall region by turbulent motions stay a long time, since the intensity of the normal component of the velocity is very small [93].

Since a large number of particles *almost* reach the wall, even a modest force acting on these particles might be enough to make them deposit. Therefore, the inclusion of lift forces, van der Waals forces and Brownian motion is crucial in modeling and simulation of soot deposition. Brownian diffusion generally dominates over the turbulence dispersion effect in the region closest to the wall [97], where the buildup of a high concentration of particles leads

to an increase in the deposition by diffusion with time [98].

Intermediate-sized particles in the near-wall region in a turbulent flow will have a better chance of getting all the way to the wall by actually first escaping the viscous sublayer [95]. This is due to that the large gradient in normal fluctuating velocity in the buffer region forms a 'trap' for particles with too little inertia to cross through all the way to the wall [99], if they are too large to effectively diffuse the last distance by Brownian diffusion.

The two different deposition mechanisms (Brownian motion and turbulence) give rise to different patterns of trapped particles on the wall [100], and are characterized by different wall impact velocities (low and high, respectively) [98].

Turbulence modeling in particle transport

In most industrial applications, it is not possible to simulate the full gas phase flow field using DNS. The application of LES to one-way coupled particle-laden turbulent channel flow was investigated by Wang & Squires [101, 102]. When compared to DNS, LES was found to be nearly as accurate. The differences to experiments were mainly found in the near-wall region, and were similar to those found between DNS and experiments, suggesting that the discrepancies might in fact stem from the description of particle motion and not the turbulent flow field itself. The best agreement between LES and DNS was found for particles with larger response times. This is due to the fact that particles with shorter response times are responsive to a broader spectrum of scales and thus are more adversely affected when the effect of subgrid-scale velocity fluctuations on particle deposition are neglected [102].

Possible ways to enhance the performance of particle tracking with LES include performing the simulations on a finer grid or introducing a model in the particle equation of motion to account for the subgrid-scale fluctuations [103]. Also the subgrid-scale model used for the gas phase plays an important role. By comparing LES results to DNS, Armenio et al. [104] concluded that the dynamic subgrid-scale model is the best choice for simulations of particle motion.

In the RANS approach, only the mean fluid velocity is resolved, so the turbulent dispersion of particles has to be modeled. The most widely used technique is to use a random-walk model, in which particles interact with a succession of stylized turbulent eddies. Random-walk models can also be used with more advanced turbulence models or any other situation where the exact and entire time history of the turbulent flow is not accessible. The random-walk technique was first applied to turbulent diffusion of particles by Yuu et al. [105], and has since been further developed by a number of

authors. The main idea is that a turbulent eddy is sampled from a Gaussian distribution based on the local turbulence quantities, and is characterized by a velocity fluctuation and a time scale. The fluid velocity experienced by the particle is taken as the sum of the mean fluid velocity and the current eddy velocity. The duration of this interaction is then the shortest of the eddy lifetime and the time it would take for the particle to cross through the eddy. After this time has elapsed, the particle enters a new idealized eddy.

Kallio & Reeks [99] used a random-walk approach to the modeling of particle deposition in turbulent duct flows, where they found very good agreement with experimental data. However, their turbulent flow was based on mean- and root mean square-profiles from experiments. The random-walk models are very sensitive to the quality of the turbulence model's prediction of the turbulent quantities. When used together with a turbulence model which is based on the assumption of isotropic turbulence (such as the $k - \varepsilon$ models), the predictions may seriously deteriorate depending on the geometry of the flow [73]. Other shortcomings of random walk models are discussed in [76]. If experimental or DNS data is available for the specific geometry of interest, the random walk model can be adjusted to take advantage of this [73]. An assumption of isotropic turbulence in the near-wall region typically leads to overpredicted deposition efficiencies [106]. Tian & Ahmadi [107] discuss in more detail the sensitivity of the predicted particle deposition behavior to the resolution of the near-wall turbulence.

Particle sticking and resuspension

The assumption that particle-surface collisions always lead to particle trapping has proven quite successful in many applications, and is referred to as the *sticky wall* boundary condition. Dahneke [108] derived an expression for the range of system properties within which particle capture will occur. In brief, the particles have to have enough energy to leave the potential well given by the van der Waals interaction energy between the particle and the surface in order to be able to bounce back from the surface, or they are trapped upon collision.

The deposition of particles at boundaries can be used to change the permeability of the computational cell at that point and/or the extension of the collecting boundary itself [cf. 109–112]. A large challenge in this type of modeling is the large separation of spatial scales between the particle and the computational cell. The trapping efficiency of a particle inside a computational cell where particles have previously deposited has to be modeled (see section 3.6.1).

The resuspension and reentrainment of particles once adhered to a sur-

face has gained almost no attention in the simulations of particle deposition in aftertreatment systems. Resuspension can be caused by fluid flow past the surface, but also be induced by other impacting particles. Theoretical models for resuspension exist, but are generally not supported by the available experimental data [113]. The need for explicit simulation of particle resuspension in trapping of diesel soot particles is not acute however, especially not inside the porous filter walls, where the flow is laminar and particle motion is eventually sterically hindered. It might be an issue in the monolith channels, but the roughness of the porous walls makes direct application of existing particle resuspension models very dubious.

Droplet-wall interaction

The droplets in a urea-spray possess more inertia than the soot particles, and will therefore reach the exhaust pipe walls mainly by inertial mechanisms. Turbulent effects, such as turbulent eddies 'throwing out' droplets against the walls, might also be important. Droplet-wall interaction in the urea-SCR system could lead to deposit formation [29, 31–38].

Birkhold et al. [114] used a wall-film model based on the work by Kuhnke [115] in CFD simulations of a urea-SCR system. Depending on temperatures and droplet deformation, droplet wall impingement may result in either film formation, wall-induced droplet breakup or bouncing back of droplets into the gas. However, the main challenge in the modeling of the droplet-wall interaction in urea-SCR systems is the complex chemistry of urea [cf. 30], where also solid deposits may be formed. Unfortunately, the wall-film models for CFD simulations available today have typically been developed for the fuel spray in the combustion chamber [115], and are therefore not directly applicable.

3.6 Approaches to particle transport in aftertreatment systems

The aim of this section is to introduce a number of important previous studies on particle transport in aftertreatment systems, in order to clearly establish the relation of the current work to what has been done before.

3.6.1 Wall-flow particulate filters

One of the oldest and most cited works in the field of modeling diesel particulate matter filtration is the '1D+'-model of Bissett [116, 117]. In this

model, the particles are assumed to be already deposited on and inside the porous wall of a wall-flow diesel particulate filter. Neglect of further particle deposition was motivated by the fact that the model is only used to study a short regeneration period [117].

Konstandopoulos & Johnson [118] presented a model for the collection efficiency of a ceramic DPF that was built on classic filtration theory. According to this model, a *unit-cell collector*, consisting of a solid sphere and an empty surrounding volume, is chosen to match the porosity of the filter material. The size of the unit collector is determined experimentally, either from mercury porosimetry or from filter permeability measurements. A deposition efficiency may then be determined from the theoretical deposition efficiency in the cell. The model has been extended to also take the effect of the previously deposited particles into account [119]. The unit cell approach has proven to be quite successful [19], most probably because it can be tuned to the material properties of the filter in question [cf. 120]. However, even if the unit cell model is fit for this purpose, it can not be used for a detailed investigation of the particle deposition process or as a means of designing new porous materials [121].

A less common alternative to the unit cell approach is based on the discrete stochastic particle deposition model of Tassopoulos et al. [122], by which the particle deposit microstructure can be correlated to a Peclet number[10] using experimental data [123]. In this way, it becomes possible to predict also the structure of the soot deposits, from which parameters such as porosity and permeability may be fed back to the wall-level in a CFD simulation.

Today, the most common approaches to modeling a DPF involve using one of the following approaches to the soot deposition process:

- An initial soot deposit layer is prescribed inside the DPF and no additional soot is trapped [124].
- Soot is assumed to deposit with a fixed[11] trapping efficiency that is chosen *a priori* [45, 125, 126].
- A pre-defined soot deposition profile that is constant in time is assumed for the filter (i.e. trapping is assumed to balance reaction) [121].
- Soot trapping is modeled with the unit cell filtration model (and the

[10] The Peclet number is a dimensionless number defined as the ratio of a characteristic time scale for diffusion (i.e. Brownian motion) to a characteristic time scale of convection.

[11] Although the fixed trapping efficiency may be chosen rather arbitrarily depending on the specific aim of the study, the most common assumption is that all incoming soot is deposited, i.e. 100%.

assumption that the particles follow the fluid streamlines all the way to the DPF wall/sootcake) [127].

- Soot particles are tracked with Lagrangian particle tracking and the deposition is modeled with a variant of the Tassopoulos et al. [122] model that is tuned to experimental data from diesel particulate filters [128].

A couple of more detailed studies of the soot deposition process has also been reported. Sbrizzai et al. [129] performed Lagrangian particle tracking for four channels of a wall-flow particulate filter. They included the drag force and the Brownian motion in their description of particle motion. After evaluating the impact velocity on the porous wall of the filter using the model by Dahneke [130], they concluded that all particles deposited upon their first impaction. A similar study on just the inlet portion of a single channel in a wall-flow filter was later presented by Liu et al. [131]. Recently, Soldati et al. [126] proposed a one-dimensional model based on lubrication theory that further elucidates the connection between filter wall permeability and homogeneity of the soot deposits.

Also the Eulerian-Eulerian multiphase model, in which the particles are treated as a second fluid phase, has been applied to the gas-solids flow in diesel particulate filters [132, 133]. In this approach, the effect of the Brownian motion on the particle trajectories is not taken into account. In addition, computational restrictions typically limit the number of particle size classes that can be used at the same time and necessitates the omission of particle-particle interactions on the drag force.

3.6.2 Flow-through particulate filters

More challenging from a modeling perspective are the simulations of particle motion in flow-through devices. Here, the extent of particle deposition is lower than in the wall-flow filters. The wall-normal gas flow velocities are also typically very low, and the predicted results therefore become much more sensitive to the accuracy of the modeling of particle motion in the gas phase [cf. 47, 129].

The extent of particle deposition in a conventional diesel oxidation catalyst was first assessed theoretically by Johnson & Kittelson [88]. They found that the deposition is negligible on a mass basis. Lylykangas & Maunula [134] showed that the residence times for particulate matter in a flow-through substrate could be prolonged with the aid of protrusions. A longer residence time would increase the conversion of the oxidation reaction of particulate matter.

Lagrangian particle tracking for a flow-through substrate was first performed by Andreassi et al. [135]. In the Lagrangian force balance, they included only the steady drag, and for the porous walls in the system they used constant trapping efficiencies.

In the current work, a detailed model for the motion and deposition of particulate matter is provided in **paper II**. A computationally more efficient *hybrid* model, which is based on the assumption that diesel and gasoline particulate matter can be divided into three distinct size classes, is then derived and evaluated in **paper III**.

3.6.3 Porous walls of particulate filters

The motion of particulate matter inside the porous walls of a diesel particulate filter using the lattice-Boltzmann technique [136] has been the focus of a number of recent studies [109, 137–142]. In these simulations, the computational mesh for the porous structure has been either created from actual measurements [140] or generated by advanced computational approaches [cf. 138, 143]. The particles themselves have however been treated as small in comparison to the spatial scales of the pores, so that there is no influence of the presence of a particle on the surrounding flow field.

In order to relate these studies to the present work, a brief discussion about the Boltzmann equation and methods pertaining to its solution is necessary. The Boltzmann equation describes the time evolution of a distribution function in particle phase space. This equation may be solved using a stochastic numerical method known as the direct simulation Monte Carlo (DSMC) method [144]. Although this allows rarefaction to be accurately handled, the computational cost is unfortunately prohibitive at small but finite Knudsen numbers [145, 146]. A more popular method is therefore to construct simplified models designed to incorporate the essential physics in the Boltzmann equation, e.g. the lattice-Boltzmann equation [136].

The lattice-Boltzmann equation is a specially discretized form of the continuous Boltzmann equation [147] (typically the Boltzmann Bhatnagar-Gross-Krook equation [148]). The purpose of the lattice-Boltzmann method has initially been to mimic continuum fluid dynamics, hence the obtained flow field is a solution to the Navier-Stokes equations [137]. For lattice-Boltzmann techniques to be extended to non-continuum regimes (i.e. finite Knudsen numbers), further development is necessary [149]. Various suggestions include modifications similar to those used when trying to extend the validity of the Navier-Stokes equations to microflows, i.e. changing the boundary conditions [150, 151] or using higher-order lattice-Boltzmann methods [152]. The latter approaches available today can provide quantitatively

correct solutions up to $Kn \sim O(1)$, but fail for higher Knudsen numbers [146].

The potential advantage of the lattice-Boltzmann technique to a conventional finite-volume technique is at present more efficient parallelization and handling of the computational mesh. In terms of accuracy at finite Knudsen numbers, promising results have been obtained but the techniques are still being developed [151]. It should also be stressed that altered boundary conditions, as a way to address the failures of the fluid flow predictions using continuum theory, have been much less successful for flow around particles than flow over plane surfaces [78, 153]. It remains to be seen what can be done within the lattice-Boltzmann framework in confined, rarefied particulate flows.

In the current work, an alternate finite-volume continuum approach that allows for accurate simulations of the flow of particles inside the pores of porous materials is proposed in **paper IV**.

3.6.4 Urea-spray droplets

Spray applications represent a class of dispersed multiphase flows where a wide range of sizes and a large number of droplets typically are present in the system at the same time. The most straightforward approach to modeling such a system is within the Lagrangian particle tracking framework, and consequently, the literature contains a great number of such studies [e.g. 39, 114, 154–157]. However, most of the focus of the previous work on the urea-SCR application has been on the decomposition chemistry and kinetics of urea. The influence of the modeling choices for the spray on the determination of reaction kinetics, or the importance of the feedback of droplet heat and mass transfer effects on the droplet motion, has previously not been studied. Therefore, the details of the modeling of the momentum, heat and mass transfer to and from urea-spray droplets are discussed in great detail in **paper I** in this thesis. For a more thorough discussion about heat and mass transfer of urea-spray droplets, the reader is also referred to [158].

Chapter 4

Results

4.1 Introduction

In this chapter, the main results from the included papers are summarized. An overview of the studies presented in this thesis is first provided in Table 4.1. The papers are characterized by which type of particles they deal with, which flow regimes are being covered and which device in the exhaust gas aftertreatment system the study is concerned with.

4.2 Paper I

In **paper I**, the urea-spray upstream a urea-SCR catalyst is investigated. A sensitivity study is carried out to determine to what extent the overall results from a typical CFD simulation of a urea-SCR system are dependent on the specific choice of sub-models for the spray.

The motion of the droplets is solved for with Lagrangian particle tracking. Using a method where the lift force, the thermophoretic force and the

Paper	**Particle type**	**Flow regime**	**Application**
I	Droplets	Turbulent	SCR
II	Particulate matter	(arbitrary)	FTF
III	Particulate matter	(arbitrary)	FTF
IV	Particulate matter	Stokes flow	DPF
V	Particulate matter	Transitional	DOC
VI	Particulate matter	Turbulent	DOC

Table 4.1: Overview of the included papers.

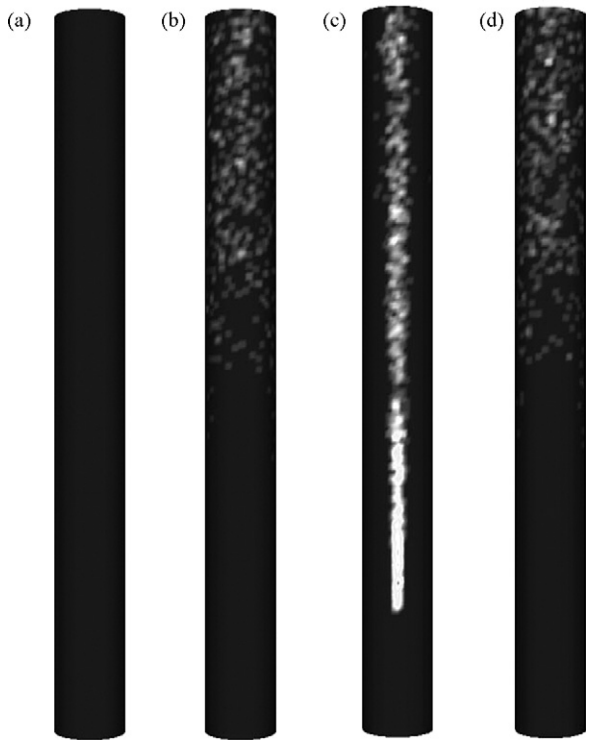

Figure 4.1: Areas of droplet wall hit for a simulation with [(c) & (d)] and without [(a) & (b)] a model for the turbulent dispersion of droplets. The side of the pipe opposite the injector [(b) & (d)] look similar, but large differences are observed on the injector side [(a) & (c)].

history force on the droplets are estimated during the course of a number of simulations, it is concluded that these forces are small compared to the drag force and the buoyancy force, and need therefore not be included. The drag force, which is the dominant force, is however sensitive to a number of sub-models, aiming at taking the current level of droplet distortion and the 'blowing effect' from the mass transfer from the droplet into account.

Turbulent dispersion is identified as being one of the greatest challenges in the modeling of droplet motion in urea-SCR systems. Since the rate of water evaporation and urea decomposition is slow compared to the retention time in the exhaust gas before the SCR-catalyst, turbulence plays a very important role both when it comes to dispersion (which is coupled to the uniformity in the ammonia concentration profiles at the inlet of the SCR-catalyst) and decomposition (since the heat and mass transfer rates are dependent on the relative velocity between the droplets and the gas). Figure 4.1 shows the sensitivity in the determination of wall impact to whether a turbulent dispersion model is included or not.

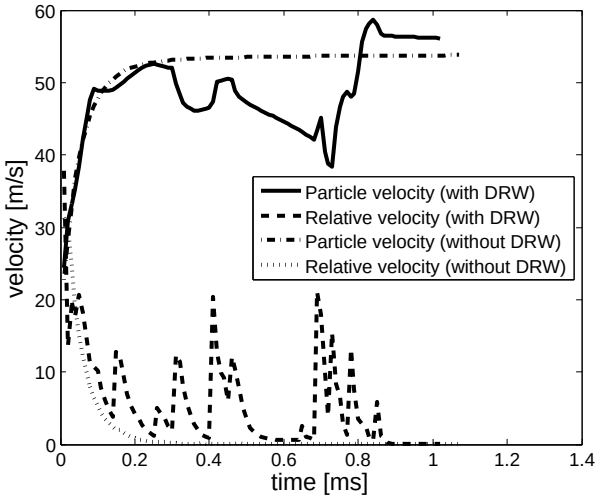

Figure 4.2: An example of droplet velocity and droplet relative velocity to the gas for a 5 μm droplet with and without a discrete random walk (DRW) model.

In Figure 4.2, it is shown that the relative velocity, and therefore also the heat and mass transfer rates, continue to vary throughout the droplet lifetime when the turbulent dispersion is taken into account.

4.3 Paper II

Paper II contains an elaborate model for Lagrangian point-particle tracking of diesel and gasoline particulate matter in flow-through devices. After a thorough literature study, a particle equation of motion for a soot particle in the limit of zero Reynolds number was assembled. This particle equation of motion contains the five most important phenomena on particle motion, modeled as five different forces.

First, there is the drag force, which here includes a Cunningham correction for non-continuum effects [81] and a drag coefficient correlation that is valid for all Reynolds numbers experienced by the particles in the system (including the deposition phase in the near wall region [93]) [159]. Then, there is the Brownian motion, which is modeled as a white-noise process [85]. The gravitational acceleration is also included, as it might influence the largest (heaviest) particles [88]. Following the recommendations of McLaughlin [93], the lift force is also included in the model. Here, the most elaborate lift force expressions from Wang et al. [160] are used, as these are valid both for strong and weak shear as well as in the core flow and in the near-wall region. Finally, the van der Waals interaction force between particles and the

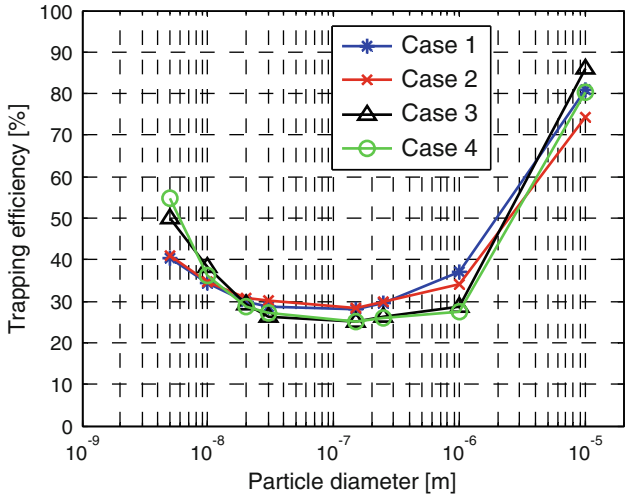

Figure 4.3: Trapping efficiency as a function of particle diameter for the geometry investigated in **paper II**. Cases 1-4 represent four different mean gas flow velocities (24, 17, 12 and 8 m s^{-1}, respectively).

surfaces of the system are included and modeled including the retardation effects [161]. The gas flow is solved for using LES with the dynamic subgrid-scale model [68, 69, 162]. In this way, the model is general and therefore applicable in its presented form to any conceivable filter design irrespective of the filter channel Reynolds number.

The proposed model is then used to track soot particles of varying properties through a flow-through filter design with protrusions. It is shown that there exists a minimum in the trapping efficiency for the intermediate-sized soot particles ($d_p \approx 150$ nm), whereas small and large particles are trapped to a higher extent. The particle trapping efficiency as a function of particle size is depicted in Figure 4.3.

Moreover, the varying sensitivity of the different sized particles to the fluid flow field and the non-continuum phenomena is shown to be reflected in the patterns created by the trapped particles on the substrate walls, as shown in Figure 4.4. Whereas the smaller particles are trapped evenly on the available surfaces, the larger particles are concentrated to areas where the fluid time scale is shortest, i.e. at the protrusions and obstacles in the flow. As different sized particles are known to have different chemical properties [10], this has important implications for soot reactivity in different parts of the flow-through device - and could also possibly be used for optimization of the distribution of e.g. noble metals in future designs.

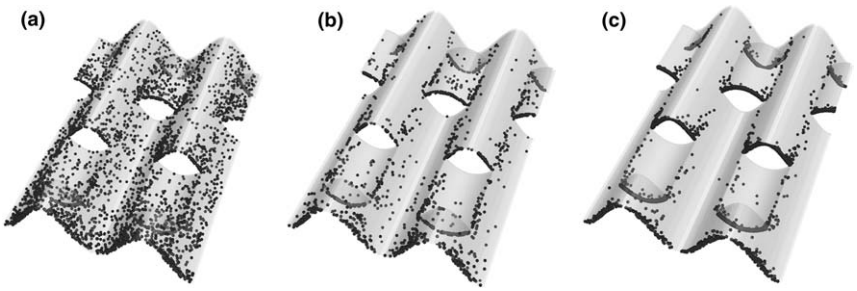

Figure 4.4: Example of patterns of particle trapping on the internal walls of the geometry investigated in **paper II**: a) 5 nm particles, b) 150 nm particles, c) 10 μm particles.

4.4 Paper III

The study reported in **paper III** deals both with model reduction and design optimization of flow-through filters.

A sensitivity study of the Lagrangian point-particle equation of motion from the model presented in **paper II** is carried out. It is shown that with little loss of generality, the **paper II**-model can be significantly reduced in complexity for the smallest particle sizes. Using an analogy between Brownian motion and diffusion [77], it is shown that the smallest particles can be represented as a diffusing pseudo-gaseous species. In addition, it is also shown that the **paper II**-model can be somewhat reduced for the largest particles, leading to a division of the particle size range into three distinct groups for which different sub-models for particle motion may be applied. This new approach is denoted a *hybrid model*. The performance of the hybrid model for a test geometry is illustrated in Figure 4.5.

Although there admittedly is a loss of generality and also of some information (e.g. deposition locations) with the hybrid model, the great advantage is a significant reduction of the computational demand of about one order of magnitude. The **paper III**-model therefore opens up for actual optimization of flow-through filter design. In particular, since the sub-model for the smallest particles is the most computationally efficient and the majority of the soot particles by number are small particles, this model may also be used as a *screening model*.

To this end, a number of different flow-through filter designs are investigated using the screening model. A comparison between six different designs is shown in Figure 4.6. In combination with the unit-cell models for particle trapping in porous media [119] and a model for soot oxidation [45], also designs with porous parts may be investigated. It is shown that a design with porous obstacles is especially interesting, as the screening indicates that it

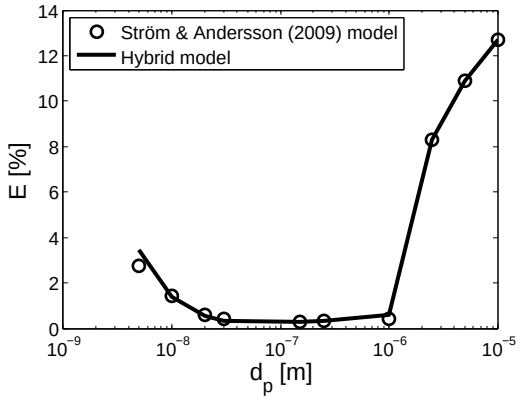

Figure 4.5: The particle trapping efficiency (E) for a test case geometry in **paper III** plotted as a function of the particle size. The proposed hybrid model is in excellent agreement (within a 95% confidence interval) with the elaborate model from **paper II**.

could be used to obtain up to 70% particle trapping efficiency of the smallest particles without imposing a substantial pressure drop. Experimental investigation will now have to be used in order to assess the performance of such a design under real-world conditions.

4.5 Paper IV

The lack of accurate modeling frameworks for the tracking of soot particles inside the pores of a porous material, such as the walls of a DPF, is the starting point for **paper IV**. The aim is to propose a modeling framework for the smallest spatial scales of diesel and gasoline particulate matter applications, that is theoretically based, in contrast to empirical approaches that have to be fit to each new system with new experimental data.

Therefore, a comprehensive model is proposed for simulations of particle motion in gas-solid systems where the sizes of the particles are significant to that of the bounding geometry and to the mean free path of the gas. The model is general in the sense that it can be used with any multiphase DNS method of choice, and it is based on a concept where the density is adjusted to account for rarefication effects. It is derived for unbounded Stokes flow. A comparison of the model to experimental data and two other theoretical approaches is shown in Figure 4.7.

In spite of the assumptions of unbounded flow in the derivation of the model, it compares favorably with much more computationally demanding DSMC simulations also for bounded geometries when compared to the alternate approach of using a slip boundary condition at the particle surface. Also

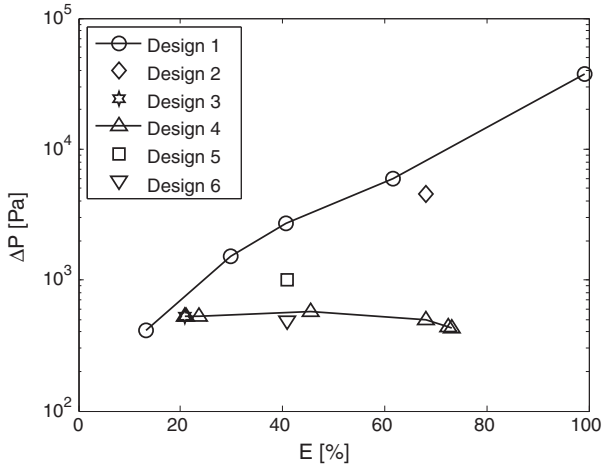

Figure 4.6: A comparison of six different designs investigated in **paper III**. The channel pressure drop (ΔP) is plotted versus the particle trapping efficiency (E) of 5 nm particles. Certain variations of Design 4 (a channel with porous obstacles) look especially interesting, as they appear to have a good balance between the obtained trapping efficiency and imposed pressure drop.

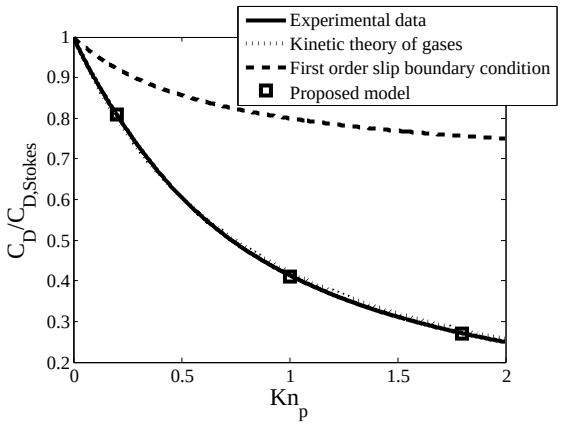

Figure 4.7: Drag reduction due to rarefaction for particle motion in an unbounded flow. Comparison between experimental data [82], kinetic theory of gases [163], Navier-Stokes equations with a first-order slip boundary condition [78] and the model proposed in **paper IV**.

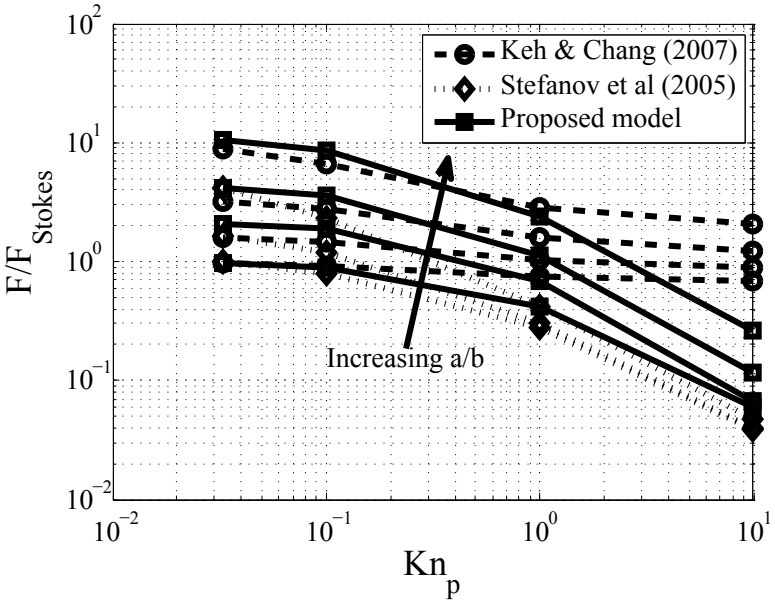

Figure 4.8: The normalized drag force on a particle accelerating in slip Poiseuille flow in a cylindrical pore. The four lines for the model proposed in **paper IV** and the results of Keh & Chang [164] correspond to particle-to-pore diameter ratios $a/b = 0$; 0.2; 0.4 and 0.6. The three lines for the DSMC results of Stefanov et al. [145] correspond to $a/b = 0$; 0.2 and 0.5.

particle-particle interactions are inherently accounted for. Figure 4.8 shows the performance of the proposed model in comparison to the slip boundary condition approach and a DSMC method for the case of an accelerating particle in a cylindrical pore.

The model presented in **paper IV** makes possible detailed investigations of the interaction between particle motion and deposition and pore geometry. It is the aim that this modeling approach will make it possible to derive mechanistic models for the events that are governing the deposition process. In this way, it will be possible to construct sub-models for the filtration process in a given porous material based only on its porous properties (e.g. pore size distribution, tortuosity, isotropy etc). In addition, it will also be possible to suggest new properties of porous materials that have not yet been manufactured, which would be beneficial for the overall filter performance.

4.6 Paper V

Paper V deals with the effects of the transition from turbulent to laminar flow in the first section of a monolithic reactor for automotive pollution con-

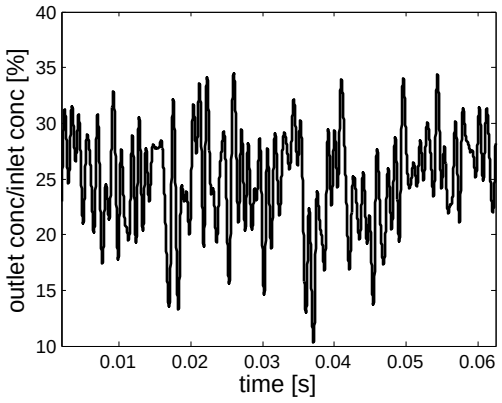

Figure 4.9: Outlet mixed-cup concentration of CO from an automotive monolithic reactor channel where the turbulent-to-laminar transition in the channel is modeled using LES (from **paper V**).

trol. The flow field is solved for using LES and the conversion of three types of species is investigated (under the assumption that conversion is mass-transfer controlled). Figure 4.9 shows how the outlet concentration of CO fluctuates in time due to the turbulence of the incoming exhaust gas flow. The power spectral density of the outlet concentration signal reveals that the dominant frequencies are approximately in the range 200 - 2000 Hz, which corresponds to the frequencies of the turbulent fluctuations at the monolith inlet. The two most dominant peaks are found at approximately 200 Hz and 800 Hz.

Two mechanisms which can explain the observations in Figure 4.9 are proposed. These are: slow fluctuations, due to turbulent eddies that are too large to enter the channel, and rapid fluctuations, due to smaller turbulent eddies that penetrate the channels. The mechanisms are illustrated schematically in Figure 4.10.

In addition, inertial 1 μm particles are tracked in the transitional flow at the monolith inlet, and it is found that they deposit on the frontal walls but only to a very low extent inside the channels. However, when deposition has occurred over a longer period of time, so that bulges have been formed at the inlet of the channel, particles may deposit also inside the channel.

4.7 Paper VI

In **paper VI**, it is suggested from correlations that a DOC operating entirely within the turbulent flow regime could exhibit a significant increase in the number trapping efficiency of particulate matter. A design criterion is proposed, from which a turbulent design that has the same conversion

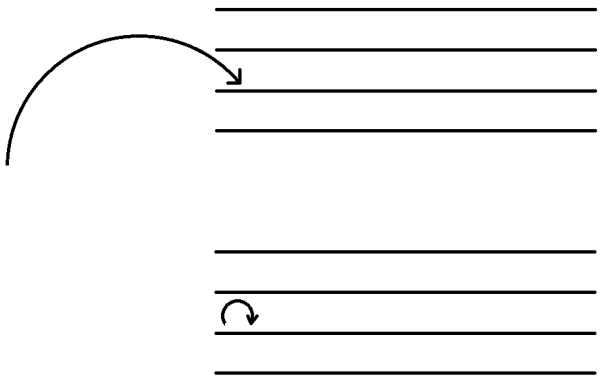

Figure 4.10: Two mechanisms by which the turbulent-to-laminar transition may effect the conversion of pollutants, as suggested in **paper V**. Above: Large turbulent eddies redirect the flow into the channels. Below: Smaller turbulent eddies penetrate the channels.

	Laminar	**Turbulent**
$d_{channel}$	1 mm	2 mm
ℓ	0.2 m	1.4 m
$U_{channel}$	10 m s^{-1}	72 m s^{-1}
Re	200	3000
ΔP	1900 Pa	48,000 Pa

Table 4.2: Comparison between a laminar and a turbulent monolith at the same conversion of gaseous pollutants at 300°C, assuming conversion is mass-transfer limited.

of gaseous pollutants as its laminar counterpart may be chosen. Table 4.2 shows a comparison between a laminar and a suggested turbulent DOC that have the same volume.

The turbulent DOC is then investigated using CFD to assess its performance. It is shown that the turbulent DOC complies with the conversion target set by the design criterion. Furthermore, LES with Lagrangian particle tracking is performed, which makes it possible to obtain the particle trapping characteristics. The deposition efficiency is significantly higher in the turbulent DOC for all particle sizes investigated (cf. Figure 4.11). For a particle size distribution representative for typical diesel exhaust, the total number trapping efficiency in the turbulent DOC is approximately 70%.

In summary, the turbulent DOC is shown to have a marked increase in the trapping efficiency of small particles compared to the laminar one, and could thus be used to target this specific particle size class and/or to optimize

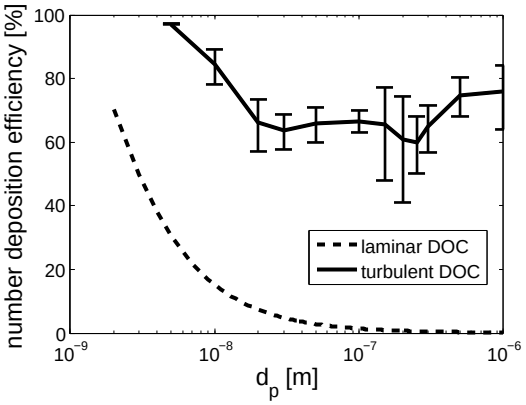

Figure 4.11: Total number trapping efficiency for particulate matter in the turbulent DOC as a function of the particle size: Comparison between the turbulent DOC (LES results) and the laminar DOC (correlation of Hawthorn [165]). The error bars indicate a 95% confidence interval for the LES results.

the performance of a combined DOC+DPF system. In order for this to be a plausible industrial solution, an assessment of the value of the decrease in regeneration frequency and the increase in DPF performance robustness must be weighted against the possible substantial increase in overall pressure drop over the combined system.

Chapter 5

Discussion

5.1 Introduction

In this chapter, three important aspects of the current work are discussed: verification, validation and qualification. The interplay between these concepts in modeling and simulation are illustrated in Figure 5.1.

By definition [11], verification is the process by which it is made certain that the solution obtained is in fact the solution to the posed problem, i.e. that the computerized model is a sufficiently accurate representation of the conceptual model. Validation is the process by which it is established whether the computerized model produces results which compare favorably with experimental findings. In model qualification, the aim is to determine whether the conceptual model is adequate for the intended level of accuracy and agreement to be obtained between computational results and experimental observations.

This chapter will start with a discussion about the numerical simulations, and then conclude with a discussion about comparisons of the current results to experimental data from the literature.

5.2 Numerical simulations

Simulations of chemical reactors involving multiphase flow and heat and mass transfer effects are rarely done on the full system level except with very crude or reduced models. In contrast, in-depth research on such systems is generally constrained to the appropriate *unit problems* into which the full system can be divided. The current work evidently deals with the unit problem of particulate flow in aftertreatment systems. For this subsystem, numerical simulations (DNS, in particular) are known to provide valuable information.

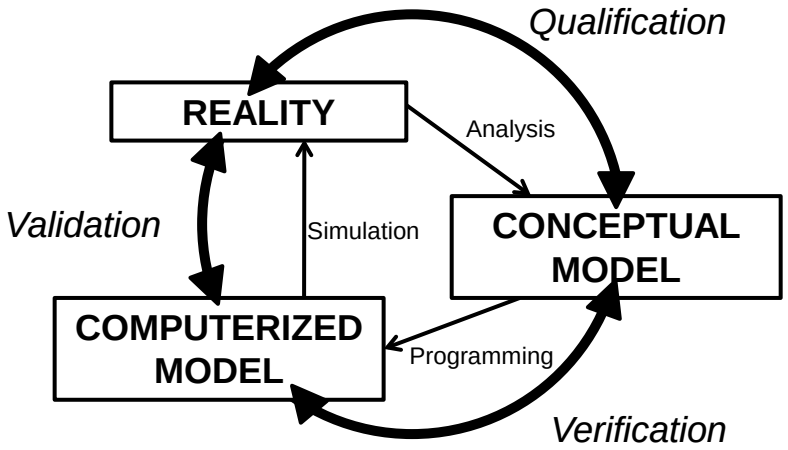

Figure 5.1: Illustration of the different phases of modeling and simulation and the roles of verification, validation and qualification [cf. 11].

It is open for discussion to what extent numerical simulations can produce information which is generally valid (i.e. to what extent the simulation results may be validated by experiments) and to what extent they merely produce a higher level of understanding and knowledge, which is necessary in the forthcoming stages of building models for the whole system.

5.2.1 Validation of CFD simulations

CFD simulations may be categorized into three levels of increasing accuracy requirements: depending on whether they are supposed to provide qualitative information, incremental quantities or absolute quantities [166]. The reason that incremental quantities can be determined with a lower degree of accuracy than absolute quantities is the effect of cancelation of errors in an incremental comparison.

The possibility of complex interactions, where multiple errors or inaccuracies may cancel one another, renders validation of a CFD code in the strictest sense almost impossible [11]. In general, code validation is often performed continually in an empirical manner, where the computational model is tested in more and more situations as reliable experimental data with well-documented experimental uncertainties becomes available. Such validation of parts of the current work is currently being planned and is discussed further in section 7.

5.2.2 Numerical experiments

As discussed in chapter 3.2, the Navier-Stokes equation and the continuity equation combined contain the exact solution to a fluid flow problem, provided that they are solved on a sufficiently fine computational mesh and with a sufficiently short time step. DNS is therefore generally referred to as a tool for *numerical experiments* [167, 168], and much of the current state-of-the art insight into particle transport phenomena has been obtained using DNS rather than experiments [92–96].

5.2.3 Influence of modeling assumptions

Whenever a numerical simulation is performed that is not a DNS, there is a certain level of approximation involved in solving the aerodynamic problem. Where LES is used in the current work, it is always with a very high resolution, in the sense that the effect of the unresolved scales on the resolved scales is small. The gas flow field obtained with LES should therefore agree well with that of a DNS.

However, when Lagrangian particle tracking is used with LES, there is also an effect of the unresolved scales on the particle motion which must be assessed. This effect is more pronounced for particles whose Stokes numbers are much smaller than unity [102]. In short, the results become sensitive to the fact that the fluid velocity as seen by the particles is in fact a modeled variant of the spatially filtered velocity, and not the actual physical velocity [169]. However, as shown by Marchioli et al. [103], it may not be sufficient to introduce the correct amount of velocity fluctuations to the velocity field experienced by the particles, as the near-wall accumulation predicted still may be inaccurate. In addition, the performance of the dynamic subgrid-scale models for LES in the dissipation range of the turbulent energy spectrum is dubious, since they tend to overpredict the subgrid-scale eddy viscosity in the limit of complete spatial resolution [170, 171].

However, the main focus of the current work is on the particle deposition process, where the events in the near-wall region are believed to be the rate-limiting step [92, 93, 95, 98]. Since whenever LES has been used, care has been taken to completely resolve the near-wall flow-field, the effects of the unresolved scales on the deposition process have been kept to a minimum.

Where RANS-based models are used for the continuous phase, it is not to be expected that absolute quantities can be obtained unless the simulation setup is tuned to experimental data for the specific flow situation. Qualitative information and incremental quantitative results for mean (averaged) properties may however be possible to obtain.

The most significant assumption made in the current work regarding the particles is most probably that they are assumed to be spherical. Deviations from the spherical shape will affect predictions of particle motion and diffusivity, and introduce a dependence of the motion on the particle orientation. In diesel particulate matter applications, the accumulation mode particles are known not to be spherical. However, it has been shown that, for the typical conditions in an aftertreatment system and the sizes of these particles, the particles will behave more or less like spheres with the same projected area [172]. In addition, the ratio of the maximum to the minimum mobility diameter for typical aerosol agglomerates is less than 1.2 [172], and effects of particle orientation are therefore small. It is thus concluded that the assumption of spherical particles is acceptable.

5.3 Experimental validation

5.3.1 Urea-SCR

The approach taken to the modeling of urea decomposition in **paper I** has recently been compared to the experimental data of Wang et al. [173] by Lundström et al. [174], and it outperforms the often cited approach taken by Birkhold et al. [156]. However, a theoretically derived model for urea evaporation has recently been proposed which compares more favorably with the experimental data [174].

The modeling approach that the evaporation of water takes place at temperatures below the melting point of urea, and the decomposition of urea only at higher temperatures, has been experimentally confirmed by Lundström et al. [175].

The model presented in **paper I** should thus be applicable if qualitative information or incremental quantities are sought for the droplet-gas interaction. For this model to provide information on the full system, a wall-film model and an approach to turbulent dispersion that have been experimentally validated for the urea-SCR system will be necessary. Simulations of an entire urea-SCR system, including the catalyst brick, are then preferably performed using the so-called *porous medium* approach [176].

5.3.2 Particle deposition efficiencies

The theoretically estimated particle deposition efficiency curve of Johnson & Kittelson [88] agrees well with the test geometry results in **paper III**. This confirms the qualitative validity of both the hybrid model and the elaborate

model, and verifies their implementation.

Experimental data on particle filtration efficiencies are more common in the literature for wall-flow filters. Yang et al. [140] measured experimentally the particle filtration efficiency from the outlet channel of a DPF with nearly spherical laboratory-generated particles. They found a minimum in the particle trapping efficiency for intermediate-sized particles (between 80 and 200 nm). Similar results, with minima around 100 nm, have been observed experimentally by Konstandopoulos & Papaioannou [19] and Bensaid et al. [177]. These results are consistent with the qualitative characteristics of particle deposition reported in the current work.

Abd-Elhady et al. [25] concluded from experiments that there exists a critical velocity, below which extensive fouling of EGR coolers takes place. The particle size in their experiments was 130 nm, with a standard deviation of 55 nm and additional smaller concentration peaks in the 10 - 100 nm range. Their conclusion, that the flow velocity past the EGR cooler should be as high as possible in order to minimize the deposition of particles, is well explained by the models presented in the current work. The results from **papers II** and **III** clearly show that for particles of this size, deposition is likely to occur mainly by Brownian motion, and that such deposition may be counteracted by an increase in the gas flow velocity past the surface.

5.3.3 Turbulent-to-laminar transition

The study on the effects of the turbulent-to-laminar transition at the inlet of a monolithic reactor in **paper V** was motivated by experimental findings. Here, the numerical simulations provide a way to obtain a deeper theoretical understanding of the phenomena of interest. Moreover, in **paper V** it is concluded that most of the deposition of inertial particles will take place on the frontal walls of the monolith. This result is supported by additional experimental observations not cited in the paper. It has for example been observed that the total inlet front face may become blocked by soot at unfavorable combinations of soot and NO_2-concentrations [54].

Chapter 6

Conclusions

In the current work, computational models for simulations of particulate flows in aftertreatment systems have been developed. These models have been used for numerical simulations, from which new insight into the flow of particles and droplets in aftertreatment systems has been obtained. The main conclusions are summarized below.

A computationally efficient hybrid model has been presented, in which the particulate matter is divided into three groups depending on their diameter. This model has been shown to be as accurate as a considerably more elaborate model (also proposed within the current work) when it comes to estimations of the particle trapping efficiency, but much more computationally efficient. Using the hybrid model, detailed investigations of the particle trapping characteristics of arbitrarily designed flow-through devices may be performed.

A sub-model to the hybrid model can be used for screening and optimization of flow-through devices. In combination with established models for particle trapping and oxidation in porous media, the screening procedure can also be used for devices with porous part. A number of different designs have been evaluated and promising candidates have been identified for prototype testing, most notably a design with porous obstacles.

The challenging task to simulate the motion of particles in pores, where the particles are significant in size both to the pore geometry and to the mean free path of the gas, has been analyzed and a novel multiphase DNS method has been proposed. Within this newly proposed framework, simulations of particle motion can be performed with higher accuracy than with a slip boundary condition approach, but at a much lower computational cost than with a molecular technique.

Results from the numerical simulations performed within the current work has elucidated the dependence of the motion of the various sizes of particulate

matter on the different mechanisms for particle transport and deposition. It has been shown that different sized particles deposit in different locations in flow-through devices, something which may be taken advantage of in flow-through filter design. Furthermore, the effect of the gas flow streamwise velocity on the deposition process has been made clear. In order to enhance or avoid deposition of particulate matter, the velocity should be either increased or decreased, depending on the particle size.

Furthermore, the effects of turbulence on the particle transport and deposition in aftertreatment systems have been studied. It is shown that a DOC operating within the turbulent flow regime will have a significant increase in the trapping of particles, at the cost of a much higher pressure drop. As the turbulent DOC may be used to target specifically the smallest fraction of diesel or gasoline particulate matter, it can become an interesting alternative in the forthcoming attempts to comply with the new, number-based emission legislation.

Chapter 7

Future work

A natural continuation of the present work is to perform experiments for the validation of the models proposed and used in **papers II** and **III**. Such experiments are currently being planned. In addition, it is also the aim to obtain experimental validation of the results from **paper VI**.

One of the main future challenges for computational models for particulate flow in flow-through devices will be the inclusion of soot migration phenomena[1] and the incorporation of possible blow-off effects during engine transients.

Further research within the field of urea-SCR, in particular the development of a wall-film model applicable to the urea-SCR system, is the focus of ongoing research in the group. Experiments will be conducted to determine the extent and location of wall-wetting. This experimental data can also be used for validation of the chosen set of CFD models and sub-models.

The forthcoming academic challenge in the research on particulate filters is to connect the particle transport and deposition on the channel scale to the transport and reaction on the wall and pore scales. Models for particulate flow, such as the ones discussed in this thesis, can provide detailed boundary conditions to sub-models for the smaller spatial scales. An in-depth understanding of the phenomena taking place on the smallest scales of the diesel particulate matter filtration devices will be necessary to construct accurate and theoretically based sub-models. However, it is only with the aid of such models that the vision of simulation-driven *a priori*-design of advanced filtration materials with optimized positioning of the catalytically active sites can eventually be realized.

Two fundamental issues that will be possible to address once a proper theoretical foundation for the discussed sub-models has been laid are the

[1]Preliminary attempts have already been carried out at the department [178].

degree of soot-catalyst contact and the ash problems. The former is known to be one of the most significant factors effecting the rate of soot oxidation and the latter is, together with thermal degradation, the most severe threat to the function of the particulate filter during ageing.

In summary, this thesis work aspires to provide important and valuable details to the engineering toolbox that will be needed to solve these upcoming issues. In addition, it can hopefully contribute to a deeper insight into the complex system that an exhaust gas aftertreatment system represents, by providing analyses of the particulate flow unit problem.

Nomenclature

Latin letters

a/b	particle-to-pore diameter ratio
C_c	Cunningham correction factor
C_D	drag coefficient
d	diameter
d_p	particle diameter
E	number deposition efficiency
g	gravitational acceleration
k	turbulent kinetic energy
ℓ	length of monolith
L	characteristic length scale
m_p	particle mass
m_f	mass of fluid displaced by particle
n	unit outward normal
p	pressure
P	mean pressure
ΔP	pressure drop
$\overline{p}$	filtered pressure
t	time
U	mean gas phase velocity
u	instantaneous gas phase velocity
$\overline{u}$	filtered gas phase velocity
u_p	particle velocity
U_r	relative velocity between particle and gas
x	spatial coordinate
x_p	particle position

Greek letters

δ	Dirac delta function
ε	turbulent dissipation rate
λ	mean free path of the gas
μ	gas phase molecular viscosity
μ_t	gas phase turbulent viscosity
ρ	gas phase density
ρ_p	particle density
τ_p	particle response time
τ_s	system characteristic time scale
ω	turbulent specific dissipation rate

Subscripts and superscripts[1]

$'$	fluctuating quantity
$channel$	monolith channel
i	coordinate direction ($i = 1, 2, 3$)
j	coordinate direction ($j = 1, 2, 3$)
$Stokes$	Stokes flow regime

Dimensionless numbers

$Kn = \lambda / L$	Knudsen number
$Kn_p = 2\lambda / d_p$	particle Knudsen number
$Re = \rho L U / \mu$	Reynolds number
$Re_p = \rho d_p U_r / \mu$	particle Reynolds number
$St = \tau_p / \tau_s$	Stokes number

[1] Einstein notation is used throughout this thesis.

Acknowledgements

This work has been performed within the Competence Centre for Catalysis, which is financially supported by Chalmers University of Technology, the Swedish Energy Agency and the member companies: AB Volvo, ECAPS AB, Haldor Topsøe A/S, Saab Automobile Powertrain AB, Scania CV AB and Volvo Car Corporation AB.

This thesis is the result of a close collaboration with a number of people who in various ways have contributed to the final result. I therefore want to thank:

My examiner and supervisor Professor Bengt Andersson, for giving me the opportunity to do my PhD work in your group, for your always equally impressive clear-sightedness and enthusiasm in scientific discussions, and your unpretentious attitude.

My co-supervisor Associate Professor Srdjan Sasic, for your continuous support and encouragement, for being an amazing supervisor and mentor, and for your wisdom both within and without the world of research.

My colleague Andreas Lundström, for being the most outstanding source of positive energy and for sharing your skills and time so unselfishly with me.

Furthermore, I would like to thank *all* my present and former colleagues at the Department of Chemical Engineering and the Competence Centre for Catalysis for making this a very nice workplace. Thanks to Love for introducing me to the C3SE clusters. Special thanks also to my office mates over the years: Rahman, Hanna and Farideh, who put up not only with me but also with my music.

Thanks to 'my own' diploma workers: Elias, Rodrik and Ebrahim. I hope you learned as much from working with me as I did from working with you.

Many warmest thanks to my wonderful family (my mother, my father & my brother) and my other relatives, who always have supported me and believed in me. Big thanks and hugs to all great friends for always being there for me. And last, but foremost, thanks to my girlfriend Linda: your love can carry me through anything.

Bibliography

[1] European Environment Agency 2007 Transport and environment: on the way to a new common transport policy. *EEA Report No 1/2007.*

[2] Bang, J. K., Hoff, E. & Peters, G. 2008 EU Consumption, Global Pollution. *WWF-World Wide Fund For Nature.*

[3] Heywood, J. B. 1988 *Internal Combustion Engine Fundamentals.* McGraw-Hill Book Company.

[4] Petersson, G. 2006 *Kemisk miljövetenskap.* Chalmers University of Technology.

[5] Lighty, J. S., Veranth, J. M. & Sarofim, A. F. 2000 Combustion Aerosols: Factors Governing Their Size and Composition and Implications to Human Health *J. Air Waste Manage. Assoc.* **50**, 1565-1618.

[6] Report on a WHO Working Group 2003 Health Aspects of Air Pollution with Particulate Matter, Ozone and Nitrogen Dioxide. *Report on a WHO Working Group, Bonn, Germany, 13-15 January.*

[7] European Environment Agency 2007 Air pollution in Europe 1990-2004. *EEA Report No 2/2007.*

[8] Solomon, S., Qin, D., Manning, M., Chen, Z., Marquis, M., Averyt, K.B., Tignor, M. & Miller, H.L. (eds.) 2008 *IPCC, 2007: Climate Change 2007: The Physical Science Basis. Contribution of Working Group I to the Fourth Assessment Report of the Intergovernmental Panel on Climate Change.* Cambridge University Press, Cambridge, United Kingdom and New York, NY, USA.

[9] Taylor, A. M. K. P. 2008 Science review of internal combustion engines. *Energy Policy* **36**, 4657-4667.

[10] Kittelson, D. B. 1998 Engines and nanoparticles: A review. *J. Aerosol Sci.* **29**, 575-588.

[11] Oberkampf, W. L. & Trucano, T. G. 2002 Verification and validation in computational fluid dynamics. *Progr. Aerospace Sci.* **38**, 209-272.

[12] Boucher, M. 2010 Cost Saving Strategies for Engineering: Using Simulation to Make Better Decisions. *Aberdeen Group Report* 30-04-2010.

[13] Güthenke, A., Chatterjee, D., Weibel, M., Krutzsch, B., Koči, P., Marek, M., Nova, I. & Tronconi, E. 2007 Current status of modeling lean exhaust gas aftertreatment catalysts. *Adv. Chem. Eng.* **33**, 103-211.

[14] Konstandopoulos, A. G., Kostoglou, M., Vlachos N. & Kladopoulou, E. 2007 Advances in the science and technology of diesel particulate filter simulation. *Adv. Chem. Eng.* **33**, 213-275.

[15] Konstandopoulos, A. G. & Kostoglou, M. 2004 Microstructural Aspects of Soot Oxidation in Diesel Particulate Filters. *SAE Technical Paper* **01-0693**.

[16] Society of Automotive Engineers 1993 Chemical methods for the measurement of nonregulated diesel emissions. *SAE Handbook. Engines, Fuels, Lubricants, Emissions, and Noise.* **3** Society of Automotive Engineers, Warrendale, PA, 25-38.

[17] Tobias, H. J., Beving, D. E. & Ziemann, P. J. 2001 Chemical Analysis of Diesel Engine Nanoparticles Using a Nano-DMA/Thermal Desorption Particle Beam Mass Spectrometer. *Environ. Sci. Technol.* **35**, 2233-2243.

[18] Abdul-Khalek, I., Kittelson, D. & Bear, F. 1999 The Influence of Dilution Conditions on Diesel Exhaust Particle Size Distribution Measurements. *SAE Technical Paper* **01-1142**.

[19] Konstandopoulos, A. G. & Papaioannou, E. 1954 Update on The Science and Technology of Diesel Particulate Filters. *KONA Powder Particle J.* **26**, 36-65.

[20] Maricq, M. M. 2007 Chemical characterization of particulate emissions from diesel engines: A review. *J. Aerosol Sci.* **38**, 1079-1118.

[21] Zhu, L., Zhang, W., Liu, W. & Huang, Z. 2009 Experimental study on particulate and NO_x emissions of a diesel engine fueled with ultra low sulfur diesel, RME-diesel blends and PME-diesel blends. *Sci. Total Environ.* **408**, 1050-1058.

[22] Olfert, J. S., Symonds, J. P. R. & Collings, N. 2007 The effective density and fractal dimension of particles emitted from a light-duty diesel vehicle with a diesel oxidation catalyst. *J. Aerosol Sci.* **38**, 69-82.

[23] Moon, G., Lee, Y., Choi, K. & Jeong, D. 2010 Emission characteristics of diesel, gas to liquid, and biodiesel-blended fuels in a diesel engine for passenger cars. *Fuel* **89**, 3840-3846.

[24] Zheng, M., Reader, G. T. & Hawley, J. G. 2004 Diesel engine exhaust gas recirculation - a review on advanced and novel concepts. *Energy Convers. Manage.* **45**, 883-900.

[25] Abd-Elhady, M. S., Zornek, T., Malayeri, M. R., Balestrino, S., Szymkowicz, P. G. & Müller-Steinhagen, H. 2010 Influence of gas velocity on particulate fouling of exhaust gas recirculation coolers. *Int. J. Heat Mass Transfer* **54**, 838-846.

[26] Kittelson, D. B., Arnold, M. & Watts, W. F. 1999 *Review of Diesel Particulate Matter Sampling Methods.* Technical Report. University of Minnesota, Minneapolis, MN.

[27] Roy, S., Hedge, M. S. & Madras, G. 2009 Catalysis for NOx abatement. *Appl. Energy* **86**, 2283-2297.

[28] Lefebvre, A. H. 1989 *Atomization and Sprays.* Hemisphere Publishing, New York.

[29] Ball, J. C. 2001 A toxicological evaluation of potential thermal degradation products of urea. *SAE Technical Paper* **01-3621**.

[30] Schaber, P. M., Colson, J., Higgins, S., Thielen, D., Anspach, B. & Brauer, J. 2004 Thermal Decomposition (Pyrolysis) of Urea in an Open Reaction Vessel. *Thermochimica Acta* **424**, 131-142.

[31] Koebel, M., Elsener, M. & Kleeman, M. 2000 Urea-SCR: A promising technique to reduce NOx emissions from automotive diesel engines. *Catal. Today* **59**, 335-345.

[32] Koebel, M., Madia, G. & Elsener, M. 2002 Selective catalytic reduction of NO and NO_2 at low temperatures. *Catal. Today* **73**, 239-247.

[33] Fang, H. L. & DaCosta, H. F. M. 2003 Urea thermolysis and NO_x reduction with and without SCR catalysts. *Appl. Catal. B* **46**, 17-34.

[34] Strots, V. O., Santhanam, S., Adelman, B. J., Griffin, G. A. & Derybowski, E. M. 2009 Deposit Formation in Urea-SCR Systems. *SAE Technical Paper* **01-2780**.

[35] Fulks, G., Fisher, G. B., Rahmoeller, K., Wu, M.-C., D'Herde, E. & Tan, J. 2009 A Review of Solid Materials as Alternative Ammonia Sources for Lean NOx Reduction with SCR. *SAE Technical Paper* **01-0907**.

[36] Floyd, R., Kotrba, A., Martin, S. & Prodin, K. 2009 Material Corrosion Investigations for Urea SCR Diesel Exhaust Systems. *SAE Technical Paper* **01-2883**.

[37] Zheng, G., Fila, A., Kotrba, A. & Floyd, R. 2010 Investigation of Urea Deposits in Urea SCR Systems for Medium and Heavy Duty Trucks. *SAE Technical Paper* **01-1941**.

[38] Salanta, G., Zheng, G., Kotrba, A., Rampazzo, R. & Bergantim, L. 2010 Optimization of a Urea SCR System for On-Highway Truck Applications. *SAE Technical Paper* **01-1938**.

[39] Zheng, G., Palmer, G., Salanta, G. & Kotrba, A. 2009 Mixer Development for Urea SCR Applications. *SAE Technical Paper* **01-2879**.

[40] Zhan, R., Li, W., Eakle, S. T. & Weber, P. A. 2010 Development of a Novel Device to Improve Urea Evaporation, Mixing and Distribution to Enchance SCR Performance. *SAE Technical Paper* **01-1185**.

[41] Irandoust, S. 1989 *The monolithic catalyst reactor*. PhD thesis, Chalmers University of Technology.

[42] Hayes, R. E. & Kolaczkowski, S. T. 1994 Mass and heat transfer effects in catalytic monolith reactors. *Chem. Eng. Sci.* **49**, 3587-3599.

[43] Koltsakis, G. C. & Stamatelos, A. M. 1997 Catalytic Automotive Exhaust Aftertreatment. *Prog. Energy Combust. Sci.* **23**, 1-39.

[44] Farrauto, R. J. & Voss, K. E. 1996 Monolithic diesel oxidation catalysts. *Appl. Catal. B* **10**, 29-51.

[45] Kandylas, I. P. & Koltsakis, G. C. 2002 NO_2-Assisted Regeneration of Diesel Particulate Filters: A Modeling Study. *Ind. Eng. Chem. Res.* **41**, 2115-2123.

[46] Kato, A., Matsuda, S., Kamo, T., Nakajima, F., Kuroda, H. & Narita, T. 1981 Reaction between nitrogen oxide (NO_x) and ammonia on iron oxide-titanium oxide catalyst. *J. Phys. Chem.* **85**, 4099–4102.

[47] Knoth, J. F., Drochner, A., Vogel, H., Gieshoff, J., Kögel, M., Pfeifer, M. & Votsmeier, M. 2005 Transport and reaction in catalytic wall-flow filters. *Catal. Today* **105**, 598-604.

[48] Adler, J. 2005 Ceramic Diesel Particulate Filters. *Int. J. Appl. Ceram. Technol.* **2**, 429-439.

[49] Suresh, A., Khan, A. & Johnson, J. H. 2000 An Experimental and Modeling Study of Cordierite Traps - Pressure Drop and Permeability of Clean and Particulate Loaded Traps. *SAE Technical Paper* **01-0476**.

[50] Fino, D. 2007 Diesel emission control: Catalytic filters for particulate removal. *Sci. Tech. Adv. Materials* **8**, 93-100.

[51] Fino, D. & Specchia, V. 2008 Open issues in oxidative catalysis for diesel particulate abatement. *Powder Tech.* **180**, 64-73.

[52] van Setten, B. A. A. L., Makkee, M. & Moulijn, J. A. 2002 Science and technology of catalytic diesel particulate filters. *Catal. Rev.* **43**, 489-564.

[53] Liati, A. & Dimopoulos Eggenschwiler, P. 2010 Characterization of particulate matter deposited in diesel particulate filters: Visual and analytical approach in macro-, micro- and nano-scales. *Comb. Flame* **157**, 1658-1670.

[54] Brück, R., Hirth, P., Reizig, M., Treiber, P. & Breuer, J. 2001 Metal Supported Flow-through Particulate Trap; a Non-Blocking Solution. *SAE Technical Paper* **01-1950**.

[55] Ambrogio, M., Saracco, G. & Specchia, V. 2001 Combining filtration and catalytic combustion in particulate traps for diesel exhaust treatment. *Chem. Eng. Sci.* **56**, 1613-1621.

[56] Cheng, S.-W. S. 2003 Rolling Regeneration Trap for Diesel Particulate Control. *SAE Technical Paper* **01-3178**.

[57] Setiabudi, A., Makkee, M. & Moulijn, J. A. 2003 An Optimal Usage of NOx in a Combined Pt/Ceramic Foam and a Wall-Flow Monolith Filter for an Effective NOx-Assisted Diesel Soot Oxidation. *SAE Technical Paper* **01-0379**.

[58] Choi, Y., Dang, Z., Stone, R., Morril, M. & Floyd, D. 2007 New Flow-Through Trap System Targeting 50% PM Removal for Diesel Emission Control. *SAE Technical Paper* **01-0232**.

[59] Clift, R., Grace, J. R. & Weber, M. E. 1978 *Bubbles, drops, and particles.* New York: Academic Press.

[60] Torregrosa, A. J., Serrano, J. R., Arnau, F. J. & Piqueras, P. 2010 A fluid dynamic model for unsteady compressible flow in wall-flow diesel particulate filters. *Energy*, Article in Press.

[61] Maxwell, J. C. 1860 Illustrations of the dynamical theory of gases. *Phil. Mag.* **19**, 19-32.

[62] Cercignani, C. 2000 *Rarefied gas dynamics: From basic concepts to actual calculations*. Cambridge University Press.

[63] Navier, L. M. H. 1822 Mémoire sur les Lois du Mouvements des Fluides. *Mem. de l'Acad. d. Sci.* **6** 398.

[64] Stokes, C. G. 1845 On the Theories of the Internal Friction of Fluids in Motion. *Trans. Cambridge Phys. Soc.* **8**.

[65] Day, M. A. 1990 The no-slip condition of fluid dynamics. *Erkenntnis* **33**, 285-296.

[66] Versteeg, H. K. & Malalasekera, W. 1998 *An Introduction to Computational Fluid Dynamics - The Finite-Volume Method.* Addison Wesley Longman Limited, Essex.

[67] Pope, S. B. 2000 *Turbulent Flows.* Cambridge University Press.

[68] Germano, M., Piomelli, U., Moin, P. & Cabot, W. H. 1991 A dynamic subgrid-scale eddy viscosity model. *Phys. Fluids A* **3**, 1760-1765.

[69] Lilly, D. K. 1992 A proposed modification of the Germano subgrid-scale closure method. *Phys. Fluids A* **4**, 633-635.

[70] Pope, S. B. 2004 Ten questions concerning the large-eddy simulation of turbulent flows. *New J. Phys.* **6**, 1-24.

[71] Wilcox, D. C. 1998 *Turbulence Modeling for CFD.* DCW Industries.

[72] Speziale, C. G. On turbulent secondary flows in pipes of noncircular cross-section. *Int. J. Eng. Sci.* **20**, 863-872.

[73] Dehbi, A. 2008 A CFD model for particle dispersion in turbulent boundary layer flows. *Nuclear Eng. Des.*, **238**, 707-715.

[74] Maxey, M. R. & Riley, J. J. 1983 Equation of motion for a small rigid sphere in a nonuniform flow. *Phys. Fluids* **26**, 883-889.

[75] Fan, L-S. & Zhu, C. 1998 *Principles of gas-solid flows.* Cambridge University Press.

[76] Crowe, C., Sommerfeld, M. & Tsuji, Y. 1998 *Multiphase Flows with Droplets and Particles.* CRC Press LLC.

[77] Chandrasekhar, S. 1943 Stochastic Problems in Physics and Astronomy. *Rev. Modern Phys.* **15** 1-89.

[78] Bailey, C. L., Barber, R. W., Emerson, D. R., Lockerby, A. & Reese, J.M. 2005 A critical review of the drag force on a sphere in the transition flow regime. *Rarefied Gas Dynamics: 24th International Symposium.* American Institute of Physics.

[79] Cunningham, E. 1910 On the velocity of steady fall of spherical particles through fluid medium. *Proc. R. Soc. London A* **83**, 357-365.

[80] Millikan, R. A. 1910 The isolation of an ion, a precision measurment of its charge, and the correction of Stokes's law. *Science* **32**, 436-448.

[81] Davies, C. N. 1945 Definitive Equations for the Fluid Resistance of Spheres. *Proc. Phys. Soc.* **57**, 259-270.

[82] Allen, M. D. & Raabe, O. G. 1982 Re-evaluation of Millikan's oil drop data for the motion of small particles in air. *J. Aerosol Sci.* **13**, 537–547.

[83] Ford, B. J. 1992 Brownian movement in Clarkia pollen: A reprise of the first observations. *The Microscope* **40**, 235-241.

[84] Einstein, A. 1905 On the motion of small particles suspended in liquids at rest required by the molecular-kinetic theory of heat. *Ann. Phys.* **17**, 549-560.

[85] Li, A. & Ahmadi, G. 1992 Dispersion and Deposition of Spherical Particles from Point Sources in a Turbulent Channel Flow. *Aerosol Sci. Tech.* **16**, 209-226.

[86] Higham, D. J. 2001 An Algorithmic Introduction to Numerical Simulation of Stochastic Differential Equations. *SIAM Rev.* **43**, 525-546.

[87] Talbot, L., Cheng, R. K., Schefer, R. W. & Willis, D. R. 1980 Thermophoresis of particles in a heated boundary layer. *J. Fluid Mech.* **101**, 737-758.

[88] Johnson, J. E. & Kittelson, D. B. 1996 Deposition, diffusion and adsorption in the diesel oxidation catalyst. *Appl. Catal. B* **10**, 117-137.

[89] Messerer, A., Niessner, R. & Pöschl, U. 2003 Thermophoretic deposition of soot aerosol particles under experimental conditions relevant for modern diesel engine exhaust gas systems. *J. Aerosol Sci.* **34**, 1009-1021.

[90] Parsegian, V. A. 2006 *van der Waals forces: a handbook for biologists, chemists, engineers, and physicists.* New York: Cambridge University Press.

[91] Kuroki, T., Ishidate, M., Okubo, M. & Yamamoto, T. 2010 Charge-to-mass ratio and dendrite structure of diesel particulate matter charged by corona discharge. *Carbon* **48**, 184-190.

[92] Soldati, A. & Marchioli, C. 2009 Physics and modelling of turbulent particle deposition and entrainment: Review of a systematic study. *Int. J. Multiphase Flow* **35**, 827-839.

[93] McLaughlin, J. B. 1989 Aerosol deposition in numerically simulated channel flow. *Phys. Fluids A* **1**, 1211-1224.

[94] Brooke, J. W., Kontomaris, K., Hanratty, T. J. & McLaughlin, J. B. 1992 Turbulent deposition and trapping of aerosols at a wall. *Phys. Fluids A* **4**, 825-834.

[95] Brooke, J. W., Hanratty, T. J. & McLaughlin, J. B. 1994 Free-flight mixing and deposition of aerosols. *Phys. Fluids* **6**, 3404-3415.

[96] McLaughlin, J. B. 1994 Numerical Computation of Particles-Turbulence Interaction. *Int. J. Multiphase Flow* **20**, 211-232.

[97] Ounis, H., Ahmadi, G. & McLaughlin, J. B. 1991 Brownian Diffusion of Submicrometer Particles in the Viscous Sublayer. *J. Colloid Interface Sci.* **143**, 266-277.

[98] Chen, M. & McLaughlin, J. B. 1995 A New Correlation for the Aerosol Deposition Rate in Vertical Ducts. *J. Colloid Interface Sci.* **169**, 437-455.

[99] Kallio, G. A. & Reeks, M. W. 1989 A Numerical Simulation of Particle Deposition in Turbulent Boundary Layers. *Int. J. Multiphase Flow* **15**, 433-446.

[100] Ounis, H., Ahmadi, G. & McLaughlin, J. B. 1991 Dispersion and Deposition of Brownian Particles from Point Sources in a Simulated Turbulent Channel Flow. *J. Colloid Interface Sci.* **147**, 233-250.

[101] Wang, Q. & Squires, K. D. 1996 Large eddy simulations of particle-laden turbulent channel flow. *Phys. Fluids* **8**, 1207-1223.

[102] Wang, Q. & Squires, K. D. 1996 Large Eddy Simulation of Particle Deposition in a Vertical Turbulent Channel Flow. *Int. J. Multiphase Flow* **22**, 667-683.

[103] Marchioli, C., Salvetti, M. V. & Soldati, A. 2008 Appraisal of energy recovering sub-grid scale models for large-eddy simulation of turbulent dispersed flows. *Acta Mech.* **201**, 277-296.

[104] Armenio, V., Piomelli, U. & Fiorotto, V. 1999 Effect of the subgrid scales on particle motion. *Phys. Fluids* **11**, 3030-3042.

[105] Yuu, S., Yasukouchi, N., Hirosawa, Y. & Jotaki, T. 1978 Particle Turbulent Diffusion in a Dust Laden Jet. *AIChE J.* **24**, 509-519.

[106] Abuzeid, S., Busnaina, A. A. & Ahmadi, G. 1991 Wall Deposition of Aerosol Particles in a Turbulent Channel Flow. *J. Aerosol Sci.* **22**, 43-62.

[107] Tian, L. & Ahmadi, G. 2007 Particle deposition in turbulent duct flows - comparisons of different model predictions. *J. Aerosol Sci.* **38**, 377-397.

[108] Dahneke, B. 1971 The Capture of Aerosol Particles by Surfaces. *J. Colloid Interface Sci.* **37**, 342-353.

[109] Stewart, M., Rector, D., Muntean, G. & Maupin, G. A. 2004 Mechanistic Model For Particle Deposition In Diesel Particulate Filters Using The Lattice-Boltzmann Technique. *Ceramic Eng. Sci. Proc.* **25**, 437-446.

[110] Lantermann, U. & Hänel, D. 2007 Particle Monte Carlo and lattice-Boltzmann methods for simulations of gas-particle flows. *Computers Fluids* **36**, 407-422.

[111] Gschaider, B. F. W., Honeger, C. C. & Redl, C. E. P. 2004 Soot Particle Deposition within Porous Structures Using a Method of Moments - Lattice Boltzmann Approach. *Proceedings of Computational Science - ICCS 2004, 4th International Conference, Kraków, Poland, June 6-9.*

[112] Filippova, O. & Hänel, D. 1997 Lattice-Boltzmann Simulations of Gas-Particle Flow in Filters. *Computers Fluids* **26**, 697-712.

[113] Ziskind, G., Fichman, M. & Gutfinger, C. 1995 Resuspension of particulates from surfaces to turbulent flows - Review and analysis. *J. Aerosol Sci.* **26**, 613-644.

[114] Birkhold, F., Meingast, U., Wassermann, P. & Deutschmann, O. 2006 Analysis of the Injection of Urea-Water-Solution for Automotive SCR DeNOx-Systems: Modeling of Two-Phase Flow and Spray/Wall Interaction. *SAE Technical Paper* **01-0643**.

[115] Kuhnke, D. 2004 *Spray/Wall-Interaction Modelling by Dimensionless Data Analysis.* PhD thesis, Shaker Verlag, Aachen.

[116] Bissett, E. J. 1984 Mathematical model of the thermal regeneration of a wall-flow monolith diesel particulate filter. *Chem. Eng. Sci.* **39**, 1233-1244.

[117] Bissett, E. J. & Shadman, F. 1985 Thermal Regeneration of Diesel-Particulate Monolithic Filters. *AIChE J.* **31**, 753-758.

[118] Konstandopoulos, A. G. & Johnson, J. H. 1989 Wall-Flow Diesel Particulate Filters - Their Pressure Drop and Collection Efficiency. *SAE Technical Paper* **890405**.

[119] Konstandopoulos, A. G., Kostoglou, M., Skaperdas, E., Papaioannou, E., Zarvalis, D. & Kladopoulou, E. 2000 Fundamental Studies of Diesel Particulate Filters: Transient Loading, Regeneration and Aging. *SAE Technical Paper* **01-1016**.

[120] Masoudi, M., Heibel, A. & Then, P. M. 2000 Predicting Pressure Drop of Wall-Flow Diesel Particulate Filters - Theory and Experiment. *SAE Technical Paper* **01-0184**.

[121] Haralampous, O. A. & Koltsakis, G. C. 2004 Back-Diffusion Modeling of NO_2 in Catalyzed Diesel Particulate Filters. *Ind. Eng. Chem. Res.* **43**, 875-883.

[122] Tassopoulos, M., O'Brien, J. A. & Rosner, D. E. 1989 Simulation of Microstructure/Mechanism Relationships in Particle Deposition. *AIChE J.* **35**, 967-980.

[123] Konstandopoulos, A. G., Skaperdas, E. & Masoudi, M. 2002 Microstructural Properties of Soot Depostis in Diesel Particulate Traps. *SAE Technical Paper* **01-1015**.

[124] Koltsakis, G. C. & Stamatelos, A. M. 1997 Modes of Catalytic Regeneration in Diesel Particulate Filters. *Ind. Eng. Chem. Res.* **36**, 4155-4165.

[125] Piscaglia, F., Onorati, A., Rutland, C. J. & Foster, D. E. 2008 Multi-Dimensional Modeling of the Soot Deposition Mechanism in Diesel Particulate Filters. *SAE Technical Paper* **01-0444**.

[126] Soldati, A., Campolo, M. & Sbrizzai, F. 2010 Modeling nano-particle deposition in diesel engine filters. *Chem. Eng. Sci.* **65**, 6443-6451.

[127] Schejbal, M., Marek, M., Kubicek, M. & Koci, P. 2010 Modelling of diesel filters for particulates removal. *Chem. Eng. J.* **154**, 219-230.

[128] Zuccaro, G., Lapenta, G., Ferrero, F. & Maizza, G. 2011 Multiphase and multiphysics particle in cell simulation of soot deposition inside a diesel particulate filter single channel. *Computer Phys. Comm.* **182**, 347-359.

[129] Sbrizzai, F., Faraldi, P. & Soldati, A. 2005 Appraisal of three-dimensional numerical simulation for sub-micron particle deposition in a micro-porous ceramic filter. *Chem. Eng. Sci.* **60**, 6551-6563.

[130] Dahneke, B. 1995 Particle bounce or capture search for an adequate theory: I. Conservation-of-energy model for a simple collision process. *Aerosol Sci. Tech.* **23**, 25-39.

[131] Liu, Y., Gong, J., Fu, J., Cai, H. & Long, G. 2009 Nanoparticle motion trajectories and deposition in an inlet channel of wall-flow diesel particulate filter. *J. Aerosol Sci.* **40**, 307-323.

[132] Bensaid, S., Marchisio, D. L., Fino, D., Saracco, G. & Specchia, V. 2010 Modelling of diesel particulate filtration in wall-flow traps. *Chem. Eng. J.* **154**, 211-218.

[133] Bensaid, S., Marchisio, D. L. & Fino, D. 2010 Numerical simulation of soot filtration and combustion within diesel particulate filters. *Chem. Eng. Sci.* **65**, 357-363.

[134] Lylykangas, R. & Maunula, T. 2002 Particle Oxidation Catalyst for Heavy-Duty Diesel Engines. *Auto Technology* **5**, 57-59.

[135] Andreassi, L., Cordiner, S., Mulone, V. & Presti, M. 2002 A Mixed Numerical-Experimental Analysis Procedure for Non-Blocking Metal Supported Soot Trap Design. *SAE Technical Paper* **01-2782**.

[136] Chen, S. & Doolen, G. D. 1998 Lattice Boltzmann method for fluid flows. *Ann. Rev. Fluid Mech.* **30**, 329-364.

[137] Muntean, G. G., Rector, D., Herling, D., Lessor, D. & Khaleel, M. 2003 Lattice-Boltzmann Diesel Particulate Filter Sub-Grid Modeling - A Progress Report. *SAE Technical Paper* **01-0835**.

[138] Konstandopoulos, A. G., Kostoglou, M., Vlachos, N. & Kladopoulou, E. 2005 Progress in Diesel Particulate Filter Simulation. *SAE Technical Paper* **01-0946**.

[139] Hayashi, H. & Kubo, S. 2008 Computer simulation study on filtration of soot particles in diesel particulate filter. *Computers Math. Appl.* **55**, 1450-1460.

[140] Yang, J., Stewart, M., Maupin, G., Herling, D. & Zelenyuk, A. 2009 Single wall diesel particulate filter (DPF) filtration efficiency studies using laboratory generated particles. *Chem. Eng. Sci.* **64**, 1625-1634.

[141] Yamamoto, K., Satake, S. & Yamashita, H. 2009 Microstructure and particle-laden flow in diesel particulate filter. *Int. J. Thermal Sci.* **48**, 303-307.

[142] Yamamoto, K., Oohori, S., Yamashita, H. & Daido, S. 2009 Simulation on soot deposition and combustion in diesel particulate filter. *Proc. Combust. Inst.* **32**, 1965-1972.

[143] Koci, P., Novak, V., Stepanek, F., Marek, M. & Kubicek, M. 2010 Multi-scale modelling of reaction and transport in porous catalysts. *Chem. Eng. Sci.* **65**, 412-419.

[144] Wagner, W. 1992 A Convergence Proof for Bird's Direct Simulation Monte Carlo Method for the Boltzmann Equation. *J. Stat. Phys.* **66**, 1011-1044.

[145] Stefanov, S. K., Barber, R. W., Ota, M. & Emerson, D. R. 2005 Comparison between Navier–Stokes and DSMC calclations for low Reynolds number slip flow past a confined microsphere. *Rarefied Gas Dynamics: 24th International Symposium.* American Institute of Physics.

[146] Kim, S. H., Pitsch, H. & Boyd, I. D. 2008 Accuracy of higher-order lattice Boltzmann methods for microscale flows with finite Knudsen numbers. *J. Comput. Phys.* **227**, 8655-8671.

[147] He, X. & Luo, L.-S. 1997 A priori derivation of the lattice Boltzmann equation. *Phys. Rev. E* **55**, R6333-R6336.

[148] Bhatnagar, P. L., Gross, E. P. & Krook, M. 1954 A Model for Collision Processes in Gases. I. Small Amplitude Processes in Charged and Neutral One-Component Systems. *Phys. Rev.* **94**, 511-525.

[149] Toschi, F. & Succi, S. 2005 Lattice Boltzmann method at finite Knudsen numbers. *Europhys. lett.* **69**, 549-555.

[150] Benzi, R., Biferale, L., Sbragaglia, M., Succi, S. & Toschi, F. 2006 Mesoscopic modelling of heterogeneous boundary conditions for microchannel flows. *J. Fluid Mech.* **548**, 257-280.

[151] Sbragaglia, M. & Succi, S. 2006 A note on the lattice Boltzmann method beyond the Chapman-Enskog limits. *Europhys. lett.* **73**, 370-376.

[152] Shan, X., Yuan, X.-F. & Chen, H. 2006 Kinetic theory representation of hydrodynamics: a way beyond the Navier-Stokes equation. *J. Fluid Mech.* **550**, 413-441.

[153] Bailey, C. L., Barber, R. W. & Emerson, D. R. 2004 Is it safe to use Navier–Stokes for gas microflows? *European Congress on Computational Methods in Applied Sciences and Engineering.* ECCOMAS.

[154] van Helden, R., Verbeek, R., Willems, F. & van der Welle, R. 2004 Optimization of Urea SCR deNOx Systems for HD Diesel Engines. *SAE Technical Paper* **01-0154**.

[155] Chen, M. & Williams, S. 2005 Modelling and Optimization of SCR-Exhaust Aftertreatment Systems. *SAE Technical Paper* **01-0969**.

[156] Birkhold, F., Meingast, U., Wassermann, P. & Deutschmann, O. 2007 Modeling and simulation of the injection of urea-water-solution for automotive SCR $DeNO_x$-systems. *Appl. Catal. B.* **70**, 119-127.

[157] Munnannur, A. & Liu, Z. G. 2010 Development and Validation of a Predictive Model for DEF Injection and Urea Decomposition in Mobile SCR DeNOx Systems. *SAE Technical Paper* **01-0889**.

[158] Lundström, A. 2009 *Urea Decomposition for Urea-SCR Applications. Experimental and Computational Fluid Dynamics Studies.* PhD thesis, Chalmers University of Technology.

[159] Morsi, S. A. & Alexander, A. J. 1972 An investigation of particle trajectories in two-phase flow systems. *J. Fluid Mech.* **55**, 193-208.

[160] Wang, Q., Squires, K. D., Chen, M. & McLaughlin, J. B. 1997 On the role of the lift force in turbulence simulations of particle deposition. *Int. J. Multiphase Flow* **23**, 749-763.

[161] Gregory, J. 1981 Approximate Expressions for Retarded van der Waals Interaction. *J. Colloid Interface Sci.* **83**, 138-145.

[162] Kim, S.-E. 2004 Large Eddy Simulation Using an Unstructured Mesh Based Finite-Volume Solver. *34th AIAA Fluid Dynamics Conference and Exhibit 2004* **2548**, 1-7.

[163] Beresnev, S. A., Chernyak, V. G. & Fomyagin, G. A. 1990 Motion of a spherical particle in a rarefied gas. Part 2. Drag and thermal polarization. *J. Fluid Mech.* **219**, 405-421.

[164] Keh, H. J. & Chang, Y. C. 2007 Creeping motion of a slip spherical particle in a circular cylindrical pore. *Int. J. Multiphase Flow* **33**, 726-741.

[165] Hawthorn, R. D. 1974 Afterburner catalysts - effects of heat and mass transfer between gas and catalyst surface. *AIChE Symp. Ser.* **137**, 428-438.

[166] Benek, J. A., Kraft, E. M. & Lauer, R. F. 1998 Validation Issues for Engine-Airframe Integration. *AIAA J.* **36**, 759-764.

[167] Orlandi, P. & Leonardi, S. 2001 DNS: a tool for numerical experiments. *in: Turbulence Structure and Modulation* (eds: A. Soldati & R. Monti), Springer-Verlag: Wien New York.

[168] Moin, P. & Mahesh, K. 1998 Direct Numerical Simulation: A tool in Turbulence Research. *Ann. Rev. Fluid Mech.* **30**, 539-578.

[169] Kuerten, J. G. M. & Vreman, A. W. 2005 Can turbophoresis be predicted by large-eddy simulation? *Phys. Fluids* **17**, 011701.

[170] Voke, P. R. 1996 Subgrid-Scale Modelling at Low Mesh Reynolds Number. *Theoret. Comput. Fluid Dynamics* **8**, 131-143.

[171] Meneveau, C. & Lund, T. S. 1997 The dynamic Smagorinsky model and scale-dependent coefficients in the viscous range of turbulence. *Phys. Fluids* **9**, 3932-3934.

[172] Rogak, S. N., Flagan, R. C. & Nguyen, H. V. 1993 The Mobility and Structure of Aerosol Agglomerates. *Aerosol Sci. Tech.* **18**, 25-47.

[173] Wang, T. J., Baek, S. W., Lee, S. Y., Kang, D. H. & Yeo, G. K. 2009 Experimental Investigation on Evaporation of Urea-Water-Solution Droplets for SCR Applications. *AIChE J.* **55**, 3267-3276.

[174] Lundström, A., Waldheim, B., Ström, H. & Westerberg, B. 2010 Modeling of Urea Gas Phase Thermolysis and Theoretical Details on Urea Evaporation. *Submitted.*

[175] Lundström, A., Andersson, B. & Olsson, L. 2009 Urea thermolysis studied under flow reactor conditions using DSC and FT-IR. *Chem. Eng. J.* **150**, 544-550.

[176] Tamaldin, N., Roberts, C. A. & Benjamin, S. F. 2010 Experimental Study of SCR in a Light-Duty Diesel Exhaust to Provide Data for Validation of a CFD Model Using the Porous Medium Approach. *SAE Technical Paper* **01-1177**.

[177] Bensaid, S., Marchisio, D. L., Russo, N. & Fino, D. 2009 Experimental investigation of soot deposition in diesel particulate filters. *Catal. Today* **147**, S295-S300.

[178] Bernerskog, E. 2007 *Deposition and migration of particulate matter in the diesel oxidation catalyst: model development and multiphase fluid dynamics.* MSc thesis, Chalmers University of Technology.